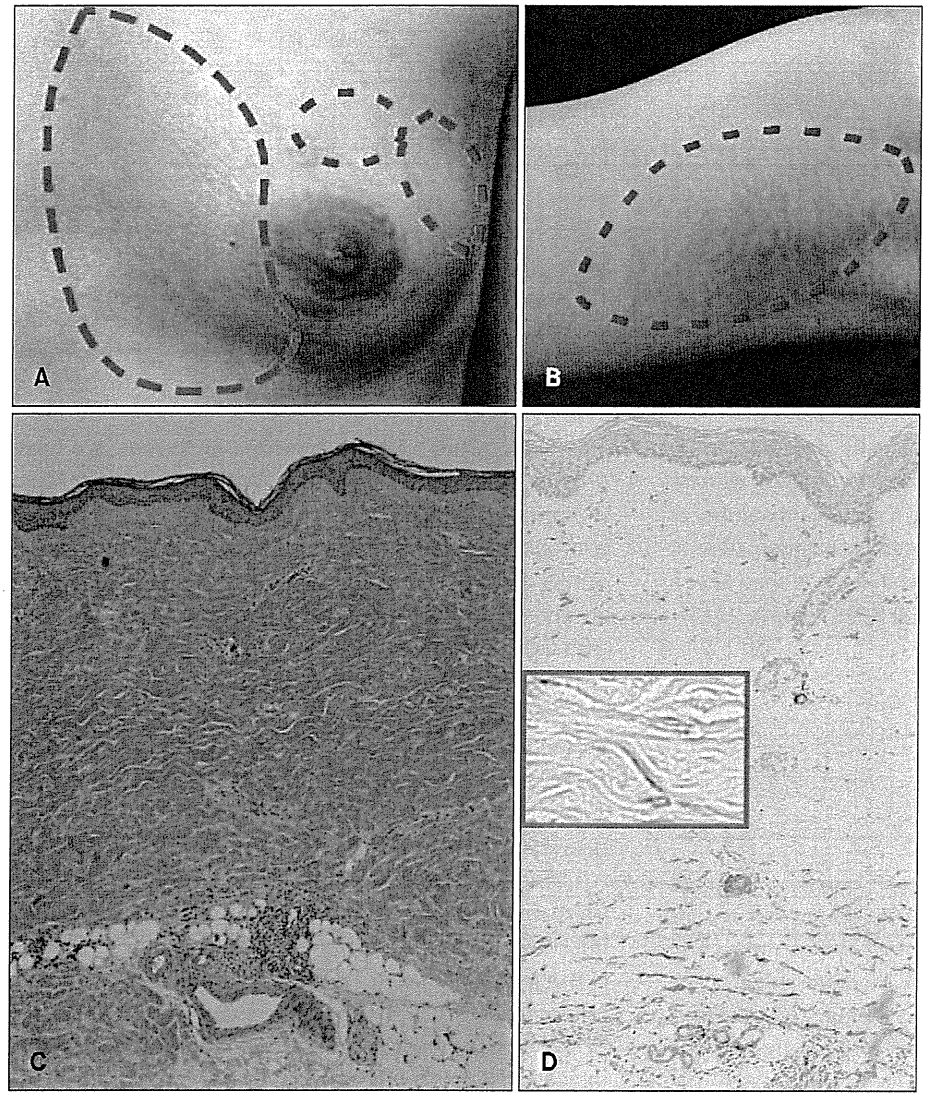

Fig. 1. (A) Morphea on the left breast (red-circle). (B) Morphea on the right upper arm (red-circle). (C) Sclerotic lesion shows thickened reticular dermis consisting of closely packed, homogenous collagen bundles with only a few fibroblasts (H&E, ×20). (D) Alpha-smooth muscle actin-positive cells were observed within the lower reticular dermis (×40).

infections and a *Borelia* infection[4]), Bacille Calmette-Guerin vaccination, pregnancy, implantation of a silicon prosthesis, viral factors, toxic factors, and neurogenic factors[5]. Christianson et al. reviewed 191 patients with localized scleroderma and showed occurrences after trauma (7.3%) and operative procedures (2.6%)[6].

Although there is a report that morphea occurred on the site of a penicillin and a local anesthetic injection[7,8], in the present case, the morphea developed after a simple physical aseptic needle aspiration without drug infusion. In a previous report, morphea had also developed on the site of an aseptic surgical examination by abdominal laparoscopy in a 56-year-old female patient[2]. These observations strongly suggest that external physical stimuli can cause morphea. The precise mechanisms underlying these phenomena are unknown. Some speculations include that trauma may trigger the production and release of inflammatory mediators and/or fibrogenic cytokines, such as transforming growth factor-beta, from cells in the microenvironment of the traumatic lesion. This can result in the synthesis of excess collagen in susceptible individuals and lead to sclerosis at a local site[9]. The reason why sclerosis but not fibrosis is induced with external stimuli and causes morphea in specific patients should be clarified in future studies.

REFERENCES

1. Terao M, Murota H, Song M, Katayama I. Case of morphea occurring on a scar after laparoscopy. J Dermatol 2006;33: 722-723.
2. Schaffer JV, Carroll C, Dvoretsky I, Huether MJ, Girardi M.

Postirradiation morphea of the breast presentation of two cases and review of the literature. Dermatology 2000;200: 67-71.
3. Kreft B, Wohlrab J, Radant K, Danz B, Marsch WC, Fiedler E. Unrecognized radiation-induced localized scleroderma: a cause of postoperative wound-healing disorder. Clin Exp Dermatol 2009;34:e383-384.
4. Zollinger T, Mertz KD, Schmid M, Schmitt A, Pfaltz M, Kempf W. Borrelia in granuloma annulare, morphea and lichen sclerosus: a PCR-based study and review of the literature. J Cutan Pathol 2010;37:571-577.
5. Ghersetich I, Teofoli P, Benci M, Innocenti S, Lotti T. Localized scleroderma. Clin Dermatol 1994;12:237-242.
6. Christianson HB, Dorsey CS, Kierland RR, O'leary PA. Localized scleroderma; a clinical study of two hundred thirty-five cases. AMA Arch Derm 1956;74:629-639.
7. Tosti A, Manuzzi P, Bardazzi F. Isomorphic phenomenon in morphea. Dermatologica 1988;177:192.
8. Ueda T, Niiyama S, Amoh Y, Katsuoka K. Linear scleroderma after contusion and injection of mepivacaine hydrochloride. Dermatol Online J 2010;16:11.
9. Yamanaka CT, Gibbs NF. Trauma-induced linear scleroderma. Cutis 1999;63:29-32.

Pigment Cell Melanoma Res. 25; 219–230

ORIGINAL ARTICLE

Dysregulation of melanocyte function by Th17-related cytokines: significance of Th17 cell infiltration in autoimmune vitiligo vulgaris

Yorihisa Kotobuki[1,2,*], Atsushi Tanemura[1,*], Lingli Yang[1,2], Saori Itoi[1], Mari Wataya-Kaneda[1], Hiroyuki Murota[1], Minoru Fujimoto[2], Satoshi Serada[2], Tetsuji Naka[2] and Ichiro Katayama[1]

1 Department of Dermatology Integrated Medicine, Osaka University Graduate School of Medicine, Osaka, Japan **2** Laboratory for Immune Signal, National Institute of Biomedical Innovation

CORRESPONDENCE Atsushi Tanemura, e-mail: tanemura@derma.med.osaka-u.ac.jp
*These authors contributed equally to this work.

KEYWORDS vitiligo/Th17 cell/Th17-related cytokines/melanocyte/interaction with skin-resident cells

PUBLICATION DATA Received 19 July 2011, revised and accepted for publication 30 November 2011, published online 3 December 2011

doi: 10.1111/j.1755-148X.2011.00945.x

Summary

The aim of this study was to determine whether CD4$^+$IL-17A$^+$Th17 cells infiltrate vitiligo skin and to investigate whether the proinflammatory cytokines related to Th17 cell influence melanocyte enzymatic activity and cell fate. An immunohistochemical analysis showed Th17 cell infiltration in 21 of 23 vitiligo skin samples in addition to CD8$^+$ cells on the reticular dermis. An in vitro analysis showed that the expression of MITF and downstream genes was downregulated in melanocytes by treatment with interleukin (IL)-17A, IL-1β, IL-6, and tumor necrosis factor (TNF)-α. Treatment with these cytokines also induced morphological shrinking in melanocytes, resulting in decreased melanin production. In terms of local cytokine network in the skin, IL-17A dramatically induced IL-1β, IL-6, and TNF-α production in skin-resident cells such as keratinocytes and fibroblasts. Our results provide evidence of the influence of a complex Th17 cell-related cytokine environment in local depigmentation in addition to CD8$^+$ cell-mediated melanocyte destruction in autoimmune vitiligo.

Introduction

In the epidermis, the epidermal melanin unit is reliant on the close interaction between a melanocyte and the associated pool of keratinocytes, and several inflammatory cytokines affect melanocyte migration, proliferation, and differentiation. Therefore, the local skin microenvironment generated by the skin-resident cells may be considered a crucial milieu for the normal life and functions of epidermal melanocytes (Chalraborty and Pawelek, 1993).

Vitiligo, a representative depigmented skin disorder associated with melanocyte destruction, affects an estimated 1% of the world's population (Howitz et al., 1977). Although the cellular immunoresponse, mainly of CD8$^+$ cytotoxic T cells, to the melanocyte-specific proteins MART-1, tyrosinase (TYR), and TRPs-1 and -2 has been shown to destroy functional melanocytes in

Significance

Here we show that not only cytotoxic T cells, which have been thought to play a major role in autoimmune vitiligo, but also infiltration of Th17 cells may play a role in vitiligo skin. In fact, we find that in vitro, a network of Th17 cell-related cytokines directly affect melanocyte activity and function, including downregulation of melanin production and shrinkage of melanocytes. These observations may shed light on the functional significance of TH17 cells in autoimmune vitiligo.

autoimmune vitiligo, this does not provide a full explanation for the etiology of vitiligo (Norris et al., 1994; Ogg et al., 1998; Okamoto et al., 1998; Ongenae et al., 2003). In addition to the autoimmune mechanism, recent reports have shown that there is a significant increase in the expression of inflammatory cytokines in affected skin compared with unaffected skin, and several investigators have proposed that the influence of local cytokines may be related to the induction and maintenance of vitiligo (Basak et al., 2009; Moretti et al., 2002, 2009; Ratsep et al., 2008). Although the representative cytokines increased in vitiligo skin have been reported to include interleukin (IL)-2, tumor necrosis factor (TNF)-α, and interferon (IFN)-γ (Caixia et al., 1999), there is no direct evidence of their function in the melanocyte destruction observed in vitiligo.

Upon induction by transforming growth factor (TGF)-b and IL-6, a subset of $CD4^+$ helper T cells develops as Th17 cells (Diveu et al., 2008). IL-17A is a cystine-linked homodimeric proinflammatory cytokine produced by Th17 cells, which form a distinct subset of the $CD4^+$ T-cell lineage. IL-17A stimulates the production of IL-1β, TNF-α, and IL-6 (Kolls and Linden, 2004; Liang et al., 2006). In the past decade, Th17 cells have been identified in autoimmune skin inflammatory disorders such as psoriasis and atopic dermatitis (Asarch et al., 2008; Fitch et al., 2009). A recent study showed a positive correlation between serum IL-17 levels and the extent of the depigmentation patch area in vitiligo, thus suggesting that Th17 cells, rather than regulatory T cells, are involved in vitiligo (Basak et al., 2009). Another study demonstrated elevated IL-17 levels in lesional skin and serum of patients with vitiligo compared with those of controls (Bassiouny and Shaker, 2011). These results indicated the importance of the secreted cytokine environment surrounding vitiliginous melanocytes in terms of vitligo etiology. In the present study, we investigated whether Th17 cells infiltrate vitiligo skin as in cases of psoriasis and whether the proinflammatory cytokines produced by Th17 cells, keratinocytes, and fibroblasts are altered in vitiligous lesions in a series of non-segmental vitiligo patients. The Th17-related cytokines tested included IL-17A and IL-22, in addition to IL-1β and IL-6, which have been reported to inhibit melanocyte activity (Kamaraju et al., 2002; Kholmanskikh et al., 2010).

MITF-M (microphthalmia-associated transcription factor-M) is a master transcription factor regulating melanocyte fate and melanogenic activity; it is distinctly expressed in melanocytes and mast cells (Levy et al., 2006). MITF expression and phosphorylation are important for the regulation of melanogenesis and melanocyte survival because the target genes of MITF encode the apoptosis regulator protein, B-cell lymphoma 2 (Bcl-2), in addition to melanogenic enzymes, tyrosinase, tyrosinase-related protein-1 (TRP-1), and dopachrome tautomerase (DCT), which are indispensable for maintaining melanocyte function (Levy et al., 2006). Because of the reduction in active melanocytes expressing these proteins in the vitiligo epidermis, the dysregulation of MITF expression has to be resolved to effectively treat vitiligo. In addition, the mRNA levels of *MITF* and *BCL2* were decreased in the lesional skin compared with the non-lesional skin of vitiligo patients (Kingo et al., 2008). The expression levels of IL-6 and TNF-α were also significantly higher in the lesional skin, indicating that in vitiligo lesions, there is increased expression of cytokines that are paracrine inhibitors of melanocytes (Moretti et al., 2002, 2009). These cytokines are produced mainly by keratinocytes, so it is possible that these cells may be abnormal in vitiligo. In addition, the expression of cytokines was unchanged in healthy skin compared with non-lesional skin, suggesting that the change observed in vitiligo lesional skin is possibly related to, or contributes to, depigmentation. Therefore, it is conceivable that there is a previously unrecognized mechanism involved in the regulation of the pigmentation-hypopigmentation balance in addition to a cytotoxic effect by $CD8^+$ T cell.

In this study, we examined the direct effect of Th17-related cytokines on MITF expression to determine the effects on the resulting cytokine involvement on the regulation of critical melanocyte behavior. We discuss the significance of Th17 cell infiltration in autoimmune vitiligo skin and propose a functional involvement of Th17 cell-related proinflammatory cytokines in vitiligo.

Results

Vitiligo skin develops in association with Th17 cell infiltration

Approval for this study was obtained from the Institutional Review Board of the Osaka University Hospital. To investigate whether Th17 cells infiltrate vitiligo skin, we performed immunostaining for IL-17A and CD4 using specific antibodies. Th17 cells were defined as the cells expressing both markers after exclusion of gamma delta T cells. Twenty-three vitiligo patients were enrolled in this study (see Table 1 for details) and were divided into 17 generalized, four localized, and two seg-

Table 1. Patients' characteristics and the infiltration status of Th17 cells

Age	27–81			
Gender				
Female	13			
Male	10			
Disease duration (yr)	0.1–26			
Mean	6.2			
	(n)	>50/field	<50/field	Not detected
Th17 cell infiltration				
Generalized type	17	11	6	0
Segmental type	4	2	0	2
Localized type	2	2	0	0
Total	23	15	6	2

mental types. The ages of the enrolled patients ranged from 27 to 81 yr, and the subjects included 13 women and 10 men. As a representative case, we show a 79-yr-old man who had experienced enlarging symmetrical depigmented macules on the whole body including face starting 2 yr previously who was positive for antithyroid antibody in the blood test (Figure 1).

Biopsy specimens were obtained from the leading edge of lesional skin on the left upper arm and were processed for the designated immunostaining. The immunohistochemical analysis revealed significant infiltration of IL-17A$^+$CD4$^+$ cells, that is, Th17 cells, mainly on the reticular dermis and perivascular region (Figure 1A). IL-17A expression was confirmed by RT-PCR using vitiligo tissue RNA. Psoriasis skin, a representative skin disease with Th17 cell infiltration, was loaded as a positive control for RT-PCR (Figure 1A). CD8$^+$ T cells were also observed, mainly below the epidermis, whereas Foxp3$^+$ cells and CD20$^+$ B cells had only faintly infiltrated (Figure 1B). Melan-A positive melanocytes were not observed in the vitiligo epidermis with inflammatory cell infiltration, whereas they were frequently located in the non-lesional skin (Figure 1B lower right panel and Inbox, respectively).

We observed a significant number of Th17 cells in 21 of 23 of the patient skin samples, and more than 50 double-positive cells per high power field were observed in 15 patients, while there was sparse infiltration in normal skin. Th17 cells were not detected in the two cases of localized type. Psoriatic skin was used as a positive control for this staining and showed the involvement as dense infiltration through the epidermis and upper dermis of pathogenic inflammatory cells whose localization was different from that in vitiligo (Figure 1C). Although we suspected that early onset and generalized type vitiligo had more opportu-

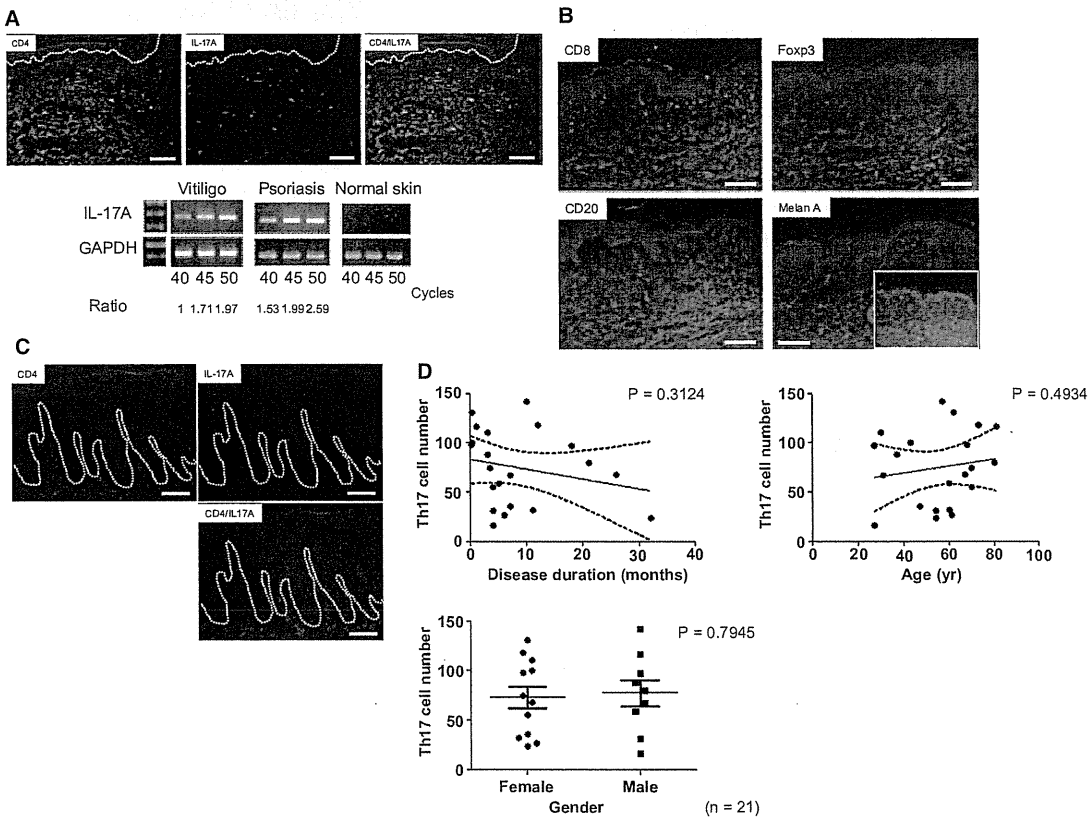

Figure 1. Photographic features of a representative generalized vitiligo patient and the immunohistochemical analysis for infiltrating cells in vitiligo skin. Multiple- and symmetrical-depigmented macules were present on the face and upper arm. A spindle-shaped skin specimen was obtained from the leading edge of an upper arm lesion. Immunostaining for CD4 and IL-17A in the vitiligo skin lesion indicated the significant infiltration of Th17 cells (yellow) positive for both CD4 (green) and IL-17A (red) mainly on reticular dermis and perivascular region. RT-PCR confirmed the same level of IL-17A expression in the vitiligo skin as in psoriasis skin (A). CD8-positive cytotoxic T lymphocytes (CTLs) (red, upper left) infiltrated the upper dermis and epidermis, whereas Foxp3 and CD20 positive cells (upper right and lower left) were only faintly detected. Melan-A-positive cells, highly differentiated melanocytes, were present in the normal region (lower right, small window), whereas they were absent in the vitiligo epidermis (lower right) (B). Psoriatic skin showed Th17 cell infiltration in the papillary dermis in addition to the epidermis (C). All images are original magnification ×40 for vitiligo and ×100 for psoriatic skin. The white bar indicates 100 μm. (D) The mean Th17 cell number present in vitiligo skin was counted on three independent fields, and the correlation with disease parameters such as disease duration, age, and gender was evaluated (n = 16).

nity to be infiltrated by Th17 cells, there was no significant correlation between the number of infiltrating Th17 cells and the clinical type, or with disease parameters such as disease duration, age, or gender in 21 patients with Th17 cell infiltration (Figure 1E).

Proinflammatory cytokines associated with Th17 cells influence in melanin activity

Because a significant number of Th17 cells were found in most of the vitiligo skin samples examined in this study, we hypothesized that there was a possible role for Th17 cell-related cytokines in melanocyte activity. Previous reports have shown that several cytokines downregulated tyrosinase activity through the activation of designated intracellular signaling pathways (Englaro et al., 1999; Kamaraju et al., 2002; Kholmanskikh et al., 2010). We therefore decided to examine the effects of IL-1β, IL-6, IL-17A, and IL-22, which are important cytokines induced by Th17 cell differentiation and maintenance, on melanocyte development and activity. MITF, a pivotal transcription factor related to melanocyte function and survival, expression and translocation was at first examined by immunocytochemistry (Figure 2A, C). Whereas there was apparent translocation of the MITF protein to the nucleus in untreated cultured melanocytes (Figure 2A), the MITF expression was decreased in the nucleus of the melanocytes treated with 10 ng/ml of IL-1β or IL-17A (Figure 2B, C), suggesting that there was a reduction in MITF-related signaling in melanocytes following cytokine treatment. In contrast, IL-22 treatment had no effect on melanocytes (data not shown), so we decided not to include IL-22 in the further experiments.

Next, we examined the expression of cytokine receptors by RT-PCR to confirm the ligand-to-receptor correspondence in melanocytes. Cultured human melanocytes were found to express IL-1R1, IL-6R, and IL-17RA without the addition of cytokines, whereas treatment with 10 ng/ml of their corresponding

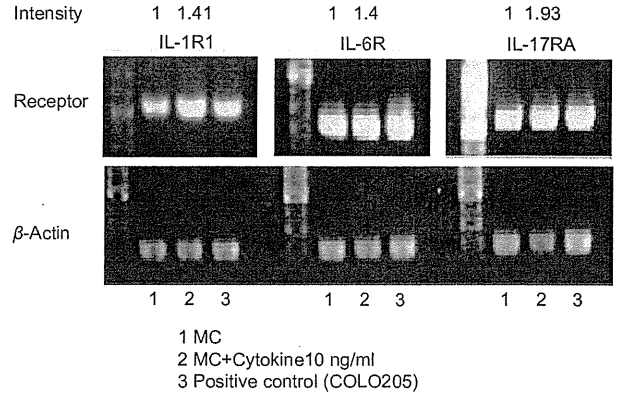

Figure 3. The expression of cytokine receptors in human melanocytes. IL-1R1, IL-6R, and IL-17RA mRNA were expressed in human melanocytes and were upregulated following treatment with their corresponding cytokines. COLO205 cells (colon cancer cell line) were used as a positive control. β-actin was used as a housekeeping gene.

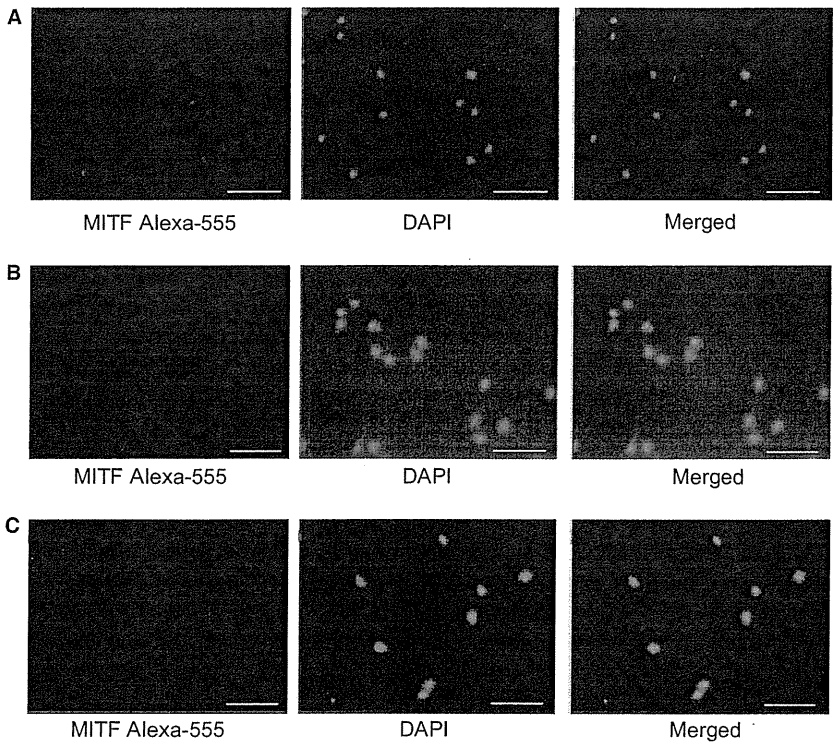

Figure 2. Immunocytochemical staining for MITF in human melanocytes. MITF was expressed mainly in the nuclei of untreated cells (A). In contrast, MITF expression was decreased after treatment with recombinant IL-1β (B) and IL-17A (C). The white bar indicates 50 μm.

cytokines increased receptor expression (Figure 3). COLO205 cells, the human colon cancer cell line expressing these receptors endogenously, were loaded in parallel with cultured melanocytes as a positive control.

To investigate the direct effects of Th17 cell-related cytokines on melanocytes in vitro, we examined the mRNA expression of melanogenic and melanocyte survival molecules after treatment of human melanocytes with recombinant human cytokines (Figure 4). The expression of *MITF*, which encodes a master transcription factor that regulates melanocyte function; of *TYR*, *TRP-1*, and *DCT*, which encode enzymes involved in melanin synthesis; and of *BCL2*, which encodes an anti-apoptotic protein, was measured by quantitative PCR. MITF expression was found to be significantly decreased in a dose-dependent manner after treatment with IL-1β, IL-6, and TNF-α (Figure 4A). The *MITF* transcription level decreased to <50% after treatment with 1 ng/ml of TNF-α. MITF was downregulated by 10 ng/ml IL-17A. In terms of the expression of its downstream enzymes, IL-1β significantly downregulated the genes, but only at a concentration of 10 ng/ml, whereas basic FGF upregulated their expression. IL-6 downregulated *TYRP1* and *DCT*, but there was no significant decrease in *TYR*. A 10 ng/ml concentration of IL-17A was needed to induce their significant downregulation. On the other hand, TNF-α significantly suppressed the expression of

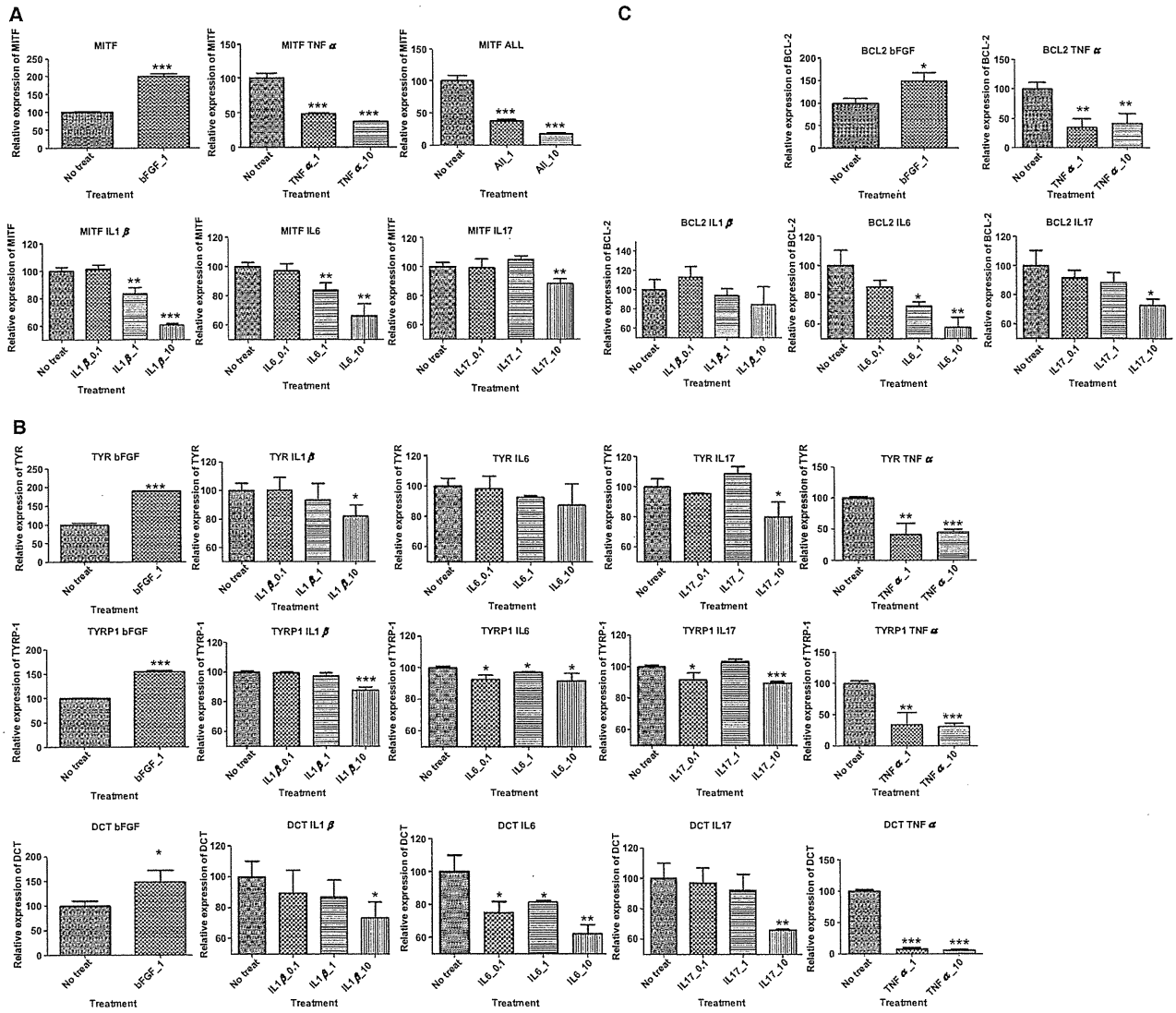

Figure 4. The quantitative analysis of the mRNA expression of MITF and genes encoding melanogenic enzymes. Human melanocytes were incubated with recombinant cytokines for 4 h at concentrations of 0.1, 1, or 10 ng/ml in the culture medium. The mRNA expression levels of MITF (A), genes encoding melanogenic enzymes (B), and B-cell lymphoma 2 (Bcl-2) (C) were measured by qRT-PCR. *P < 0.05; **P < 0.01; ***P < 0.001 compared with the expression level in untreated control cells.

these genes and *BCL2*, even at the concentration of 1 ng/ml, suggesting that TNF-α likely had the strongest suppressive effect on gene expression. BCL2 expression was decreased following treatment with IL-1β, IL-6, and IL-17A in a dose-dependent manner. Overall, there was a tendency for molecules related to melanocyte function to be downregulated following treatment with exogeneous cytokines (Figure 4B, C).

To determine the direct effects of Th17 cells on melanocytes, we performed coculture of the Th17 cells induced from peripheral blood mononuclear cells by an in vitro protocol with and without TGF-β treatment (Wilson et al., 2007) with melanocytes and real-time PCR. Th17-polarized cells without TGF-β decreased the expression of *MITF* and its downstream melanogenic molecules more than Th2-polarized cells did (Figure S1).

Furthermore, melanin production was measured after continuous treatment with exogenous cytokines including IL-1β, IL-6, IL-17A, and TNF-α. The percentage of melanin production was significantly lower in melanocytes treated with 1 and/or 10 ng/ml of exogenous cytokines than in untreated cells. In contrast, no reduction in total protein was observed after the addition of any of the cytokines (Figure 5). Because these cytokines are critical for the maintenance and development of Th17 cells from naïve $CD4^+$ T cells, we suggest that the presence of a specific local cytokine environment might be indispensable for Th17 cell recruitment and activation in vitiligo lesions, thereby indicating that they contribute significantly to depigmentation in addition to CTL (cytotoxic T cell) activation.

Production of cytokines by skin-resident cells

We have shown infiltration of Th17 cells in vitiligo skin and have demonstrated the inhibitory effects of Th17 cell-related cytokines on melanocyte function. As the cytokines examined in this study are produced not only by inflammatory cells but also by the surrounding cells, such as keratinocytes and fibroblasts, the source of the cytokine production was examined. We treated normal human epidermal keratinocyte (NHEK) and normal human dermal fibroblast (NHDF) cells with recombinant IL-17A and measured IL-1β, IL-6, and TNF-α production (Figure 6A, B). IL-17A exponentially increased the pro-

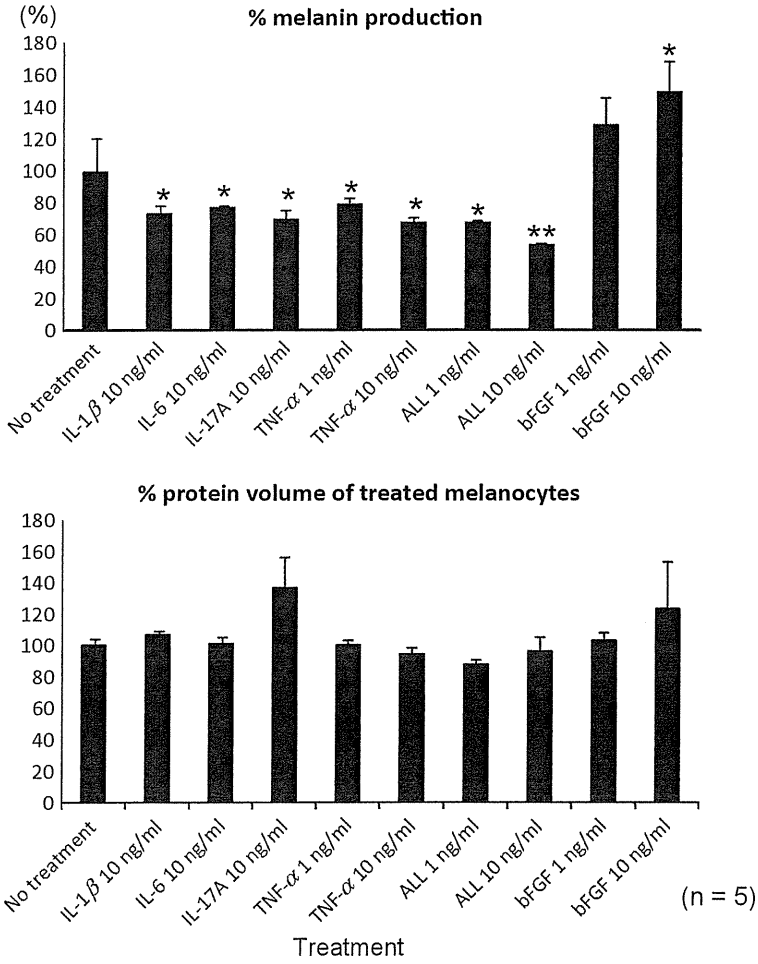

Figure 5. There is a decrease in melanin production after treatment with cytokines. Human melanocytes were incubated with 1 ng and/or 10 ng/ml of recombinant cytokines for 5 days in the culture medium (n = 5). Recombinant cytokines were added everyday. Cultured melanocytes were treated with 1 N NaOH and processed for absorbance at 450 nm to quantify the melanin volume. The protein volume of the cell extracts was measured to demonstrate whether the cytokines exerted the reduction of whole cell protein. *P < 0.05; **P < 0.01; ***P < 0.001 compared with the expression level of the untreated controls.

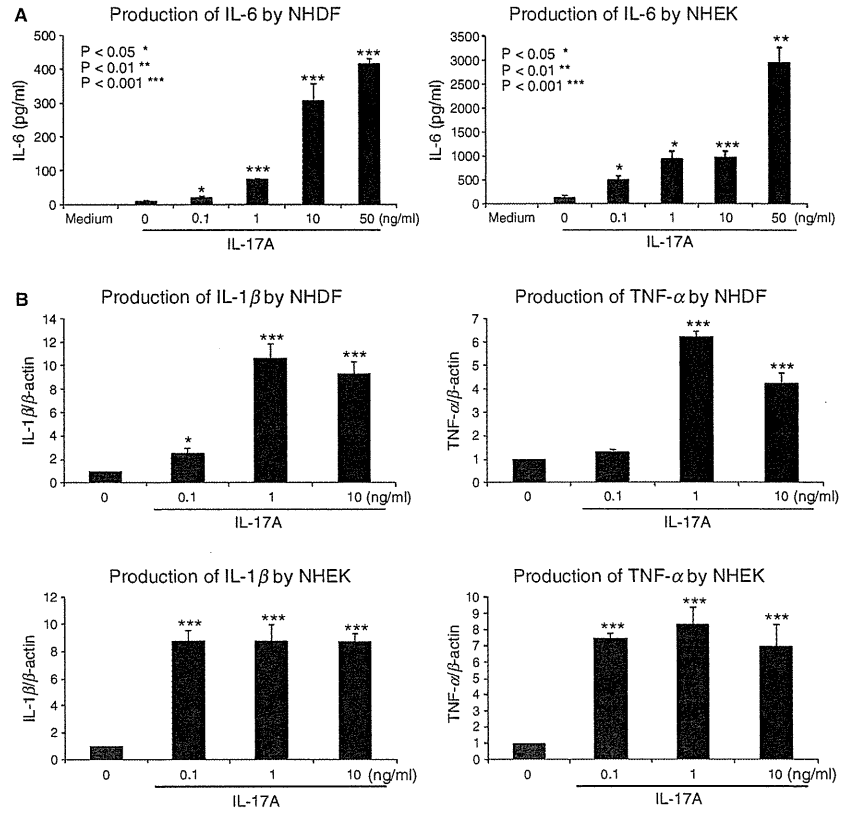

Figure 6. IL-17A induces the release of other Th17 cell-related cytokines from dermal fibroblasts and keratinocytes. (A) Human dermal fibroblasts and keratinocytes were incubated with recombinant IL-17A for 1 day at concentrations of 0.1, 1, 10, and 50 ng/ml in the culture medium, and the IL-6 secreted in the medium was measured by an ELISA. (B) After cells were incubated as in (A), the IL-1β and TNFα mRNA expression levels were measured by RT-PCR. β-actin was used as a housekeeping gene. *P < 0.05; **P < 0.01; ***P < 0.001 compared with the expression level of the untreated controls.

duction of these cytokines in a dose-dependent manner using both of these cell lines.

Cytokine-induced melanocyte dysfunction

Finally, we examined whether proinflammatory cytokines could directly induce melanocyte apoptosis and/or destruction in vitro. The cultured melanocytes were incubated with 1 and 10 ng/ml of recombinant IL-1β, IL-6, IL-17A, TNF-α, or all of the factors for 5 days, and then the melanocytes were observed microscopically under polarized light (Figure 7A). The cells were obviously aggregated and varied in shape after treatment with both the single cytokines and the cytokine cocktail, whereas the untreated cells and those treated with bFGF (basic fibroblast growth factor) grew with a spindle-shaped morphology. Staurosporine, a chemical that induces apoptosis by activating caspase-3, increased the number of round-shaped apoptotic melanocytes. TNF-α induced the greatest extent of melanocyte destruction compared with the other cytokines.

Next, melanocyte apoptosis was assessed by measuring caspase-3 activity after continuous treatment with 10 ng/ml of each of the individual cytokines and the cytokine cocktail. Staurosporine led to an increase in caspase-3 activity (Figure 7B), whereas there was no induction of caspase-3 activity following treatment with any of the cytokines. These results indicate that there appears to be direct inhibition of melanocyte activity by cytokines, rather than induction of cell apoptosis.

Discussion

In the present study, we identified a significant number of Th17 cells that had infiltrated vitiligo skin, and demonstrated the inhibitory effect of Th17 cell-related proinflammatory cytokines on melanocyte activity. We therefore hypothesize that the functional Th17 cell involvement in the initiation of psoriasis and atopic dermatitis may also play an important role in the pathogenesis of vitiligo. Although the precise pathogenic mechanisms underlying the induction of depigmentation in an immunological manner (Ongenae et al., 2003) still remain unknown, non-segmental vitiligo has been thought to be an autoimmune disease because of the high frequency of associated Hashimoto's thyroid disease (Daneshpazhooh et al., 2006; Hegedus et al., 1994; Schallreuter et al., 1994a), type I diabetes (Gould et al., 1985), collagen diseases with antinuclear antibodies (Mihailova et al., 1999), etc. Pathogenic antibodies were also detected in approximately 50% of vitiligo patients (Cui et al., 1992; Ruiz-Arguelles et al., 2007). With respect to the cellular immune condition, the infiltration of cytotoxic T cells targeting melanocyte-specific antigens in vitiligo lesions has been thought to play a critical role in hypopigmentation (Lang et al., 2001; Norris et al., 1994; Ogg et al., 1998). Recent reports have also suggested that there is the local environment of proinflammatory cytokines such as IL-1, IL-6, and TNF-α also contributes to the inhibition of melano-

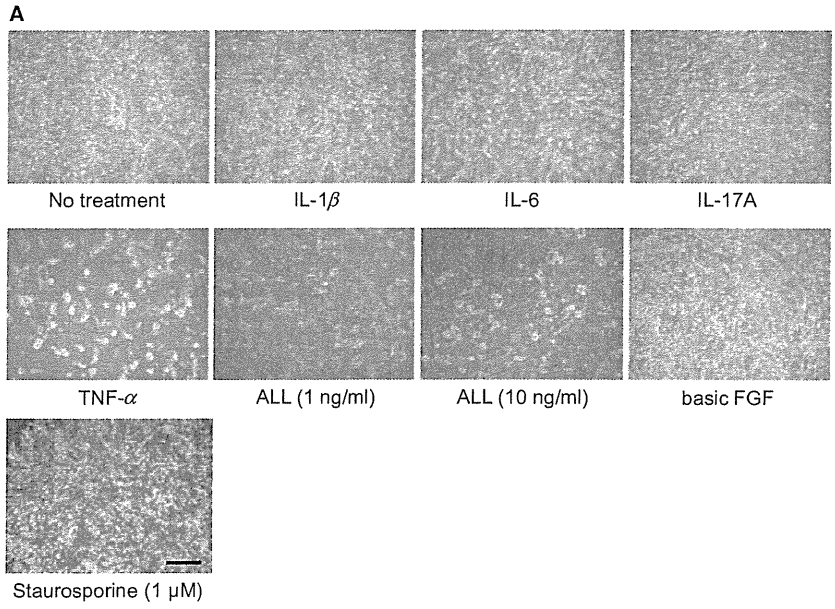

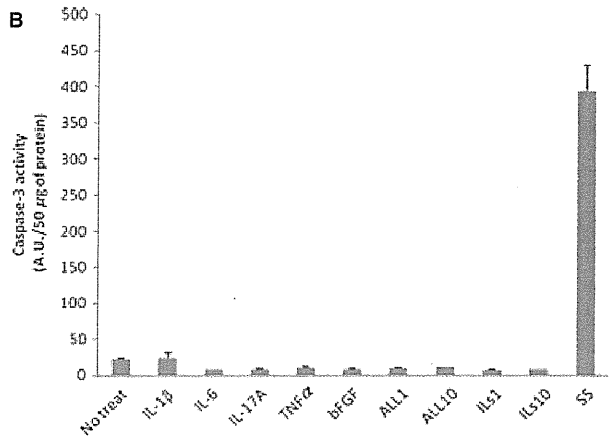

Figure 7. Proinflammatory cytokines induce melanocyte cell destruction, but not apoptosis. (A) Human melanocytes were incubated with recombinant proinflammatory cytokines, including IL-1β, IL-6, IL-17A, and TNF-α continuously for 5 days at concentrations of 1 or 10 ng/ml in the culture medium. These cytokines were used either alone or in combination. Staurosporine was used as a positive control for cell apoptosis. The photographs were taken by a polarized microscope. The bar indicates 50 μm. (B) The absorbance at 450 nm was measured to determine the caspase-3 activity of the cells treated with cytokines. ILs indicates treatment together with IL-1β, IL-6 and IL-17A.

genesis and melanocyte survival (Moretti et al., 2002, 2009).

Direct regulation of melangenic factors by cytokines

The tyrosinase mRNA levels are generally correlated with tyrosinase activity (Ando et al., 1995). In our study, cytokine treatment decreased the mRNA levels of MITF, a transcription factor implicated in regulating melanogenic and antiapoptotic genes, and decreased the expression of genes encoding melanogenic enzymes such as tyrosinase, TYRP-1, and DCT (TYRP-2) in a dose-dependent manner. These results indicate that proinflammatory cytokines can play a pivotal role in the regulation of melanocyte fate through the downregulation of gene expression.

There have been several reports providing evidence that melanocyte functions are regulated by cytokines through several cellular signaling pathways (Kamaraju et al., 2002; Kholmanskikh et al., 2010). For example, IL-1β and 1α were found to direct the downregulation of MITF-M expression through the NF-κB and JNK pathways in two different melanoma cell lines (Kholmanskikh et al., 2010). IL-6/IL-6R signaling silenced the MITF promoter activity and this was mediated by Pax3 downregulation (Kamaraju et al., 2002). IL-6 is a pleiotropic cytokine involved in a variety of inflammatory responses. With regard to the relationship to Th17 cells, IL-6 is essential for induction of Th17 cell development and maintenance (Diveu et al., 2008). As the proinflammatory cytokines involved in Th17 cell fate include IL-1β and TGF-β in addition to IL-6, we examined the expression and activity of some of these cytokines in melanocytes.

Although there is no doubt that cellular and antibody-mediated immune reactions are related to melanocyte destruction, our data suggest that Th17 cells and skin-resident cells, particularly epidermal keratinocytes and dermal fibroblasts, might orchestrate a response that inhibits the stability of melanocytes in some vitiligo skin

through the production of proinflammatory cytokines. In addition, there might be an initial trigger attracting Th17 cells to vitiligo (or pre-vitiligo) skin.

A recent study using several skin samples showed greater numbers of Th17 cells, especially on the leading edge of vitiligo skin (Wang et al., 2011). In the present study, we confirm the presence of Th17 cell infiltration in vitiligo skin and suggest that there was a pathogenic function not only because of cytotoxic T cells but also because of Th17 cells and Th17 cell-related cytokines. Although we expected that there would be more infiltration of Th17 cells in the generalized type and progressive vitiligo compared with other clinical types, there was no significant correlation between the Th17 cell number and the clinical type and disease duration. It is possible that the small sample number, biopsy site, and preceding treatments, including the use of topical steroids, may have affected the status of inflammatory cell infiltration.

We observed that Th17 cells diffusely infiltrated the upper dermis, whereas $CD8^+$ cells were present beneath the basal membrane of the epidermis. In psoriatic skin, Th17 cells mainly infiltrate into the papillary dermis and epidermis. We therefore speculated that Th17 cells might be able to act on melanocytes by producing cytokines, rather than exerting a direct effect on the cells. To address this point, we stimulated dermal fibroblasts and keratinocytes using a characteristic pro-Th17 cytokine, IL-17A. IL-17A robustly upregulated the production of IL-1β and TNF-α by these skin-resident cells, suggesting the presence of mutual cytokine signaling between skin-resident cells and accumulating inflammatory cells. The melanocytes themselves can also synthesize IL-1α and β (Swope et al., 1994).

Previous studies have shown that cytokines associated with skin inflammation, such as IL-1β, IL-6, and TNF-α, inhibited melanin production in vitro (Englaro et al., 1999; Kamaraju et al., 2002; Kholmanskikh et al., 2010). We found that there were significant changes in the expression of epidermal cytokines in vitiligo lesions, where no melanocytes are present, compared with perilesional, non-lesional and healthy skin, where melanocytes are normally present. Therefore, it is conceivable that the cytokines derived from infiltrating cells, as well as the lesional epidermis, would be implicated in depigmented skin disorders. In the present study, treatment with a physiologically relevant concentration of IL-17A, in addition to IL-1β and IL-6, could directly regulate the expression of MITF and downstream molecules, and subsequently melanin synthesis, in human melanocytes.

Putative involvement of proinflammatory cytokines in vitiligo

Based on these experimental results, we propose the putative involvement of proinflammatory cytokines in the pathogenesis of vitiligo (Figure 8). Previous studies have shown that the perforin produced from CD8-positive cytotoxic T cells (Lang et al., 2001; Norris et al., 1994; Ogg et al., 1998), antimelanocyte antibodies (Baharav et al., 1996; Cui et al., 1992; Ruiz-Arguelles et al., 2007), and reactive oxygen species were related to the injury of melanocytes and were triggers for vitiligo (Schallreuter et al., 1994b). In the present study, we found a significant infiltration of Th17 cells in vitiligo skin, and demonstrated that Th17-related cytokines such as IL-1β, IL-6, and IL-17A directly or indirectly regulated melanin production and the expression of melanogenic and antiapoptotic molecules. The presence of a cytokine network and the secretion of IL-17A from Th17 cells may therefore represent a new mechanism underlying the pathogenesis of vitiligo concerning the downregulation of melanocyte activity. Indeed, the activation of the innate immune system may lead to the accumulation of Th17 cells in the vitiligo lesion as they do in psoriasis. In fact, the IL-1β released from lesional keratinocytes and melanocytes (Moretti et al., 2002, 2009; Swope et al., 1994) may act as the first inducer of the differentiation of naïve helper T cells into Th17 cells in vitiligo lesions. Thereafter, antimicrobial peptides derived from the lesional epidermis might induce the production of IL-17A by Th17 cells (Infante-Duarte et al., 2000).

Although psoriasis is one of representative skin disorders characterized by pathogenic Th17 cell infiltration, the phenotypic change in this disorder is not akin to that in vitiligo vulgaris. Because the final targets of IL-17A in

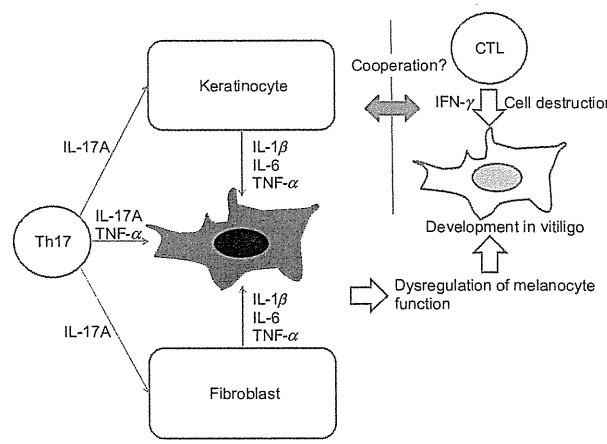

Figure 8. The proposed cues provided by Th17 cells and Th17 cell-related cytokines during the pathogenesis of autoimmune vitiligo. Previous known pathogenic mechanisms of melanocyte destruction in vitiligo include the presence of cytotoxic T cells attacking the melanocytes, local oxidative stress, and downregulation of melanogenesis-inducing factors in the vitiligo epidermis. The newly proposed phenomenon is that an imbalance in the local cytokine network is involved in the downregulation of melanocyte activity found in the present study. The IL-17A secreted from the Th17 cells in vitiligo skin can trigger the production of inhibitory cytokines from dermal fibroblasts and keratinocytes. IL-1β, IL-6, and TNF-α as well as IL17-A also repress melanocyte activity and induce melanocyte destruction.

vitiligo vulgaris and psoriasis are different, that is, melanocyte dysfunction in vitiligo vulgaris and abnormal keratinocyte turnover in psoriasis, Th17 cells may augment vitiliginous skin lesion formation in cooperation with skin-resident cells such as dermal fibroblasts and keratinocytes, as described previously. Microbial lipopeptides may then induce the cell polarization to Th17 cells, producing IL-17 and TNF-α as a result of the stimulation of the innate immune system in vitiligo (Infante-Duarte et al., 2000). Tip dendritic cell (tipCD)-like cells might also be involved in vitiligo formation, as previous reports demonstrated that the number of αDCs was increased in vitiligo vulgaris lesions or there was a unique distribution pattern of Langerhans cells present in such lesions (Mishima et al., 1972). Moreover, recent reports suggest that an altered innate immune response is observed in autoimmune vitiligo in concert with frequent *NALP1* gene mutations (Jin et al., 2007, 2010). An unrecognized micro-organism might stimulate the attending inflammatory cells through antimicrobial peptides and sequentially trigger vitiligo vulgaris. These issues should be clarified in further experiments.

Methods

Cell lines

HeMnMP, a moderately pigmented human melanocyte cell line, was obtained from Cascade Biologics and cultured in Medium 254 with human melanocyte growth supplement (Gibco Inc., Tokyo, Japan), and maintained at 37°C with 5% CO_2 in a humidified incubator. The cells were used for this study by the 5th passage to ensure melanin production. Dermal fibroblasts and epidermal keratinocytes were purchased from TAKARA BIO Inc., (Shiga, Japan) and maintained in DMEM containing 10% FCS and Medium 154 (Gibco Inc.), respectively.

Reagents

Human recombinant cytokines were purchased from Cell Signaling Technology (Tokyo, Japan) and synthetic melanin was from Sigma-Aldrich, Japan. The antibodies used for this study were as follows: anti-MITF mouse monoclonal Ab (D5) from Abcam (San Francisco, CA, USA), horseradish peroxidase (HRP)-conjugated anti-rabbit or mouse IgG from Cell Signaling Technology, anti-CD4 mouse monoclonal antibody from Novocastra Reagents (Tokyo, Japan), anti-CD8, -Foxp3, -CD20 and -Melan A mouse monoclonal antibodies from Dako (Tokyo, Japan), anti-IL17A goat monoclonal antibody from R&D (Minneapolis, MN, USA), Alexa Fluor 488-conjugated anti-mouse IgG and Alexa Fluor 555-conjugated anti-goat IgG from Invitrogen (Tokyo, Japan).

Tissue specimens

Approval for the use of human skin tissue samples was obtained from the local Ethical Committee of Osaka University Hospital and written informed consent was received from each patient after appropriate explanation of this study. Spindle-shaped skin biopsy specimens on the leading edge of vitiligo lesions were taken from 23 vitiligo patients. Twenty-three skin specimens were fixed in buffered 10% formalin and embedded in paraffin and processed for an immunohistochemical analysis as described below. Non-lesional skin from the matched vitiligo patients and normal skin from normal donors were processed as well.

RNA isolation and PCR assay for cytokine and melanocyte markers expression

Total RNA was extracted from HeMnMP cells using the TRIZOL reagent according to the manufacturer's instructions. Reverse transcription (RT) reactions were performed with Moloney murine leukemia virus reverse transcriptase (Promega, Tokyo, Japan) with oligo (dT) primers. For RT reaction of tissue RNA, total RNA was extracted from frozen vilitigo skin tissue using the Sepasol-RNA I reagent (NACALAI TESQUE, INC., Kyoto, Japan) according to the manufacturer's instructions. Genomic DNA contamination was removed by DNase I (TAKARA BIO INC.). The qRT assay was performed using an ABI prism 7900HT Sequence Detection System (Applied Biosystems, Carlsbad, CA, USA) according to the manufacturer's specifications. Briefly, the reaction mixture totaling 10 μl for each qRT consisted of 1 μl of cDNA generated from 250 ng of total RNA, 0.5 μM of Taqman probe labeled with FAM, the master mix for melanogenic markers and glyceraldehyde 3-phosphate dehydrogenase (GAPDH), or the Power SYBR green PCR master mix for cytokines. The mixture was processed by a two-step PCR method with an initial heating at 95°C for 10 min, followed by 40 cycles of denaturation at 95°C for 15 s, and annealing and extension at 60°C for 60 s for all genes. The obtained PCR amplification curves were analyzed using SDS software program, version 2.1 (Applied Biosystems). GAPDH was used as a control housekeeping gene, and the relative mRNA copy numbers were obtained as the ratio of the mRNA copies of each gene/copies of GAPDH. Each assay was performed at least three times. The specific probe and primers sequences used for this study were as follows:

MITF-M: 5′-AGCTCACAGCGTGTATTTTTCCCAC-3′
TYR: 5′-TCTCCTCTTGGCAGATTGTCTGTAG-3′
TRP-1: 5′-CTTTGTAACAGCACCGAGGATGGGC-3′
DCT: 5′-TGCAAGTGCACAGGAAACTTTGCCG-3′
BCL2: 5′-AACGGAGGCTGGGATGCCTTTGTGG-3′
GAPDH: 5′-GGGCGCCTGGTCACCAGGGCTGCTT-3′
IL-1β: Forward 5′- TGCACGCTCCGGGACTCACA-3′
IL-1 β: Reverse 5′- CGCCTTTGGTCCCTCCCAGG-3′
TNF-α: Forward 5′- CCCCTGACAAGCTGCCAGGC-3′
TNF-α: Reverse 5′- CAGCTCCACGCCATTGGCCA-3′

Reverse transcriptase PCR (RT-PCR) for IL-17A and cytokine receptor expression

To confirm IL-17A expression in vitiligo tissue and determine the expression levels of the cytokines and their receptors, we performed RT reactions with the above-mentioned procedure and PCR with an initial heating at 95°C for 10 min, followed by 40 cycles of denaturation at 95°C for 15 s, and annealing and extension at appropriate temperatures for 60 s for all genes. Samples were then processed for electrophoresis. The following primer sets were used:

IL-17A: Forward 5′- ACAAACTCATCCATCCCCAG-3′
IL-17A: Reverse 5′- GTGAGGTGGATCGGTTGTAG-3′
IL-1R1: Forward 5′-CCCGTTGCAGGAGACGGAGG-3′
IL-1R1: Reverse 5′-CCACCCAGCCAGCTGAAGCC-3′
IL-1R2: Forward 5′-CTTTAAAGCTGCTTCTGCCACGTG-3′
IL-1R2: Reverse 5′-CATTGCCCGTCCACCACAGCA-3′
IL-6R: Forward 5′-GAGTTCGGGCAAGGCGAGTGG-3′
IL-6R: Reverse 5′-AGGCTCCCTCCAGCAACCAGGAA-3′
IL-17RA: Forward 5′-AAGCCTCAGAACGTTCGTTCGCT-3′
IL-17RA: Reverse 5′-TTGGGCAGGTGGTGAACGGT-3′

Melanin content assay

Melanin production was determined as described previously (Virador et al., 1999). Briefly, 2 days after the plating of 1×10^5 melanocytes into a 6-well culture dish, we performed 5 days of

sequential treatment with 1–10 ng/ml of recombinant cytokines. To determine the melanin content, the pellets of treated cells were dissolved in 200 μl of 1 N NaOH for 30 min, and the concentrations of melanin were calculated by measuring the absorbance at 450 nm. Synthetic melanin was used to generate a standard curve. The melanin content was expressed as nanograms of melanin per microgram of total protein, and the ratio was compared among the samples.

Immunostaining

Vitiliginous skin specimens were processed after receiving written informed consent from vitiligo patients (n = 23). Paraffin-embedded archival tissues were deparaffinized with absolute xylene and dehydrated in a sequential ethanol dilution series. The deparaffinized sections were boiled in an oil bath for 15 min in 10 mM Tris-1 mM EDTA buffer (pH 9.0) for antigen retrieval. The slides were blocked by the Protein Block Serum-Free solution (Dako) for 15 min and incubated with an anti-IL-17A goat monoclonal Ab (×200) at 4°C overnight. After being washed with TBS (pH 7.6), the slides were incubated with Alexa Fluor 555-conjugated anti-goat IgG Ab (×200) and then incubated with anti-CD4 mouse monoclonal Ab (×25) at RT for 1 h, followed by incubation with Alexa Fluor 488-conjugated anti-mouse IgG Ab (×200). The following primary antibodies were used to assess the expression of melanocyte markers and the melanosomal protein MART1: anti-CD8 mouse monoclonal Ab (×25), anti-CD20 mouse monoclonal Ab (×25), anti-Foxp3 mouse monoclonal Ab (×50), and anti-Melan A (recognizing the MART-1 antigen) mouse monoclonal Ab (×50). These antibodies were provided by DAKO Inc.

For the immunocytochemistry analyses, the HeMnMP cells cultured in two-well Lab-Tek chamber slides (Nunc, Tokyo, Japan) were incubated with an anti-MITF mouse monoclonal antibody (×25) at 4°C overnight, followed by incubation with Alexa Fluor 555-conjugated anti-mouse IgG (×500) as the secondary antibody. The mouse isotype IgG was used as a negative control for staining. Nuclei were counterstained after DAPI staining (×1000).

Quantitative analysis of proinflammatory cytokines after the treatment with Th17-related cytokines

To assess the cell–cell interactions between the cells in the skin occurring as a result of paracrine cytokine production, the concentrations of proinflammatory cytokines such as IL-6 and IL-1β in the culture supernatant from dermal fibroblasts was measured 24 h after treatment with recombinant IL-17A using an ELISA kit from R&D.

Apoptosis assay

We determined the cleaved caspase-3 activity following treatment with recombinant cytokines using an apoptosis detection kit (R&D Systems). Briefly, cultured melanocytes were treated with cytokines (1 or 10 ng/ml) for 5 days. The culture medium was not changed until cell extraction, and cytokines were added in the culture medium every day. Thereafter, in addition to observation of melanocyte morphology under a polarized microscope, the melanocytes were processed for measurement of cleaved caspase-3 activity according to manufacturer's instructions.

Statistical analysis

The unpaired *t*-test was used for the analysis of differences in gene and protein expression. The results are shown as the means + SD. A value of $P < 0.05$ (two-tailed) was considered significant. All statistical analyses were performed using the PRISM software program, version 5 (GraphPad Software Inc., La Jolla, CA, USA).

Acknowledgements

We thank Kenju Nishida, Eriko Nobuyoshi, and Tomoka Matsumura for their expert technical assistance. This work was supported in part by a grant from the Ministry of Education, Culture, Sports, Science and Technology of Japan and a grant from the Ministry of Health, Labor and Welfare.

References

Ando, H., Itoh, A., Mishima, Y., and Ichihashi, M. (1995). Correlation between the number of melanosomes, tyrosinase mRNA levels, and tyrosinase activity in cultured murine melanoma cells in response to various melanogenesis regulatory agents. J. Cell. Physiol. *163*, 608–614.

Asarch, A., Barak, O., Loo, D.S., and Gottlieb, A.B. (2008). Th17 cells: a new therapeutic target in inflammatory dermatoses. J. Dermatolog. Treat. *19*, 318–326.

Baharav, E., Merimski, O., Shoenfeld, Y., Zigelman, R., Gilbrud, B., Yecheskel, G., Youinou, P., and Fishman, P. (1996). Tyrosinase as an autoantigen in patients with vitiligo. Clin. Exp. Immunol. *105*, 84–88.

Basak, P.Y., Adiloglu, A.K., Ceyhan, A.M., Tas, T., and Akkaya, V.B. (2009). The role of helper and regulatory T cells in the pathogenesis of vitiligo. J. Am. Acad. Dermatol. *60*, 256–260.

Bassiouny, D.A., and Shaker, O. (2011). Role of interleukin-17 in the pathogenesis of vitiligo. Clin. Exp. Dermatol. *36*, 292–297.

Caixia, T., Hongwen, F., and Xiran, L. (1999). Levels of soluble interleukin-2 receptor in the sera and skin tissue fluids of patients with vitiligo. J. Dermatol. Sci. *21*, 59–62.

Chalraborty, A., and Pawelek, J. (1993). MSH receptors in immortalized human epidermal keratinocytes: a potential mechanism for coordinate regulation of the epidermal-melanin unit. J. Cell. Physiol. *157*, 344–350.

Cui, J., Harning, R., Henn, M., and Bystryn, J.C. (1992). Identification of pigment cell antigens defined by vitiligo antibodies. J. Invest. Dermatol. *98*, 162–165.

Daneshpazhooh, M., Mostofizadeh, G.M., Behjati, J., Akhyani, M., and Robati, R.M. (2006). Anti-thyroid peroxidase antibody and vitiligo: a controlled study. BMC Dermatol. *6*, 3.

Diveu, C., Mcgeachy, M.J., and Cua, D.J. (2008). Cytokines that regulate autoimmunity. Curr. Opin. Immunol. *20*, 663–668.

Englaro, W., Bahadoran, P., Bertolotto, C., Busca, R., Derijard, B., Livolsi, A., Peyron, J.F., Ortonne, J.P., and Ballotti, R. (1999). Tumor necrosis factor alpha-mediated inhibition of melanogenesis is dependent on nuclear factor kappa B activation. Oncogene *18*, 1553–1559.

Fitch, E.L., Rizzo, H.L., Kurtz, S.E., Wegmann, K.W., Gao, W., Benson, J.M., Hinrichs, D.J., and Blauvelt, A. (2009). Inflammatory skin disease in K5.hTGF-beta1 transgenic mice is not dependent on the IL-23/Th17 inflammatory pathway. J. Invest. Dermatol. *129*, 2443–2450.

Gould, I.M., Gray, R.S., Urbaniak, S.J., Elton, R.A., and Duncan, L.J. (1985). Vitiligo in diabetes mellitus. Br. J. Dermatol. *113*, 153–155.

Hegedus, L., Heidenheim, M., Gervil, M., Hjalgrim, H., and Hoier-Madsen, M. (1994). High frequency of thyroid dysfunction in patients with vitiligo. Acta Derm. Venereol. *74*, 120–123.

Howitz, J., Brodthagen, H., Schwartz, M., and Thomsen, K. (1977). Prevalence of vitiligo. Epidemiological survey on the Isle of Bornholm, Denmark. Arch. Dermatol. *113*, 47–52.

Infante-Duarte, C., Horton, H.F., Byrne, M.C., and Kamradt, T. (2000). Microbial lipopeptides induce the production of IL-17 in Th cells. J. Immunol. *165*, 6107–6115.

Jin, Y., Mailloux, C.M., Gowan, K., Riccardi, S.L., Laberge, G., Bennett, D.C., Fain, P.R., and Spritz, R.A. (2007). NALP1 in vitiligo-associated multiple autoimmune disease. N. Engl. J. Med. *356*, 1216–1225.

Jin, Y., Riccardi, S.L., Gowan, K., Fain, P.R., and Spritz, R.A. (2010). Fine-mapping of vitiligo susceptibility loci on chromosomes 7 and 9 and interactions with NLRP1 (NALP1). J. Invest. Dermatol. *130*, 774–783.

Kamaraju, A.K., Bertolotto, C., Chebath, J., and Revel, M. (2002). Pax3 down-regulation and shut-off of melanogenesis in melanoma B16/F10.9 by interleukin-6 receptor signaling. J. Biol. Chem. *277*, 15132–15141.

Kholmanskikh, O., Van Baren, N., Brasseur, F., Ottaviani, S., Vanacker, J., Arts, N., Van Der Bruggen, P., Coulie, P., and De Plaen, E. (2010). Interleukins 1alpha and 1beta secreted by some melanoma cell lines strongly reduce expression of MITF-M and melanocyte differentiation antigens. Int. J. Cancer *127*, 1625–1636.

Kingo, K., Aunin, E., Karelson, M., Ratsep, R., Silm, H., Vasar, E., and Koks, S. (2008). Expressional changes in the intracellular melanogenesis pathways and their possible role in the pathogenesis of vitiligo. J. Dermatol. Sci. *52*, 39–46.

Kolls, J.K., and Linden, A. (2004). Interleukin-17 family members and inflammation. Immunity *21*, 467–476.

Lang, K.S., Caroli, C.C., Muhm, A., Wernet, D., Moris, A., Schittek, B., Knauss-Scherwitz, E., Stevanovic, S., Rammensee, H.G., and Garbe, C. (2001). HLA-A2 restricted, melanocyte-specific CD8(+) T lymphocytes detected in vitiligo patients are related to disease activity and are predominantly directed against MelanA/MART1. J. Invest. Dermatol. *116*, 891–897.

Levy, C., Khaled, M., and Fisher, D.E. (2006). MITF: master regulator of melanocyte development and melanoma oncogene. Trends Mol. Med. *12*, 406–414.

Liang, S.C., Tan, X.Y., Luxenberg, D.P., Karim, R., Dunussi-Joannopoulos, K., Collins, M., and Fouser, L.A. (2006). Interleukin (IL)-22 and IL-17 are coexpressed by Th17 cells and cooperatively enhance expression of antimicrobial peptides. J. Exp. Med. *203*, 2271–2279.

Mihailova, D., Grigorova, R., Vassileva, B., Mladenova, G., Ivanova, N., Stephanov, S., Lissitchky, K., and Dimova, E. (1999). Autoimmune thyroid disorders in juvenile chronic arthritis and systemic lupus erythematosus. Adv. Exp. Med. Biol. *455*, 55–60.

Mishima, Y., Kawasaki, H., and Pinkus, H. (1972). Dendritic cell dynamics in progressive depigmentations. Distinctive cytokinetics of -dendritic cells revealed by electron microscopy. Arch. Dermatol. Forsch. *243*, 67–87.

Moretti, S., Spallanzani, A., Amato, L., Hautmann, G., Gallerani, I., Fabiani, M., and Fabbri, P. (2002). New insights into the pathogenesis of vitiligo: imbalance of epidermal cytokines at sites of lesions. Pigment Cell Res. *15*, 87–92.

Moretti, S., Fabbri, P., Baroni, G., Berti, S., Bani, D., Berti, E., Nassini, R., Lotti, T., and Massi, D. (2009). Keratinocyte dysfunction in vitiligo epidermis: cytokine microenvironment and correlation to keratinocyte apoptosis. Histol. Histopathol. *24*, 849–857.

Norris, D.A., Horikawa, T., and Morelli, J.G. (1994). Melanocyte destruction and repopulation in vitiligo. Pigment Cell Res. *7*, 193–203.

Ogg, G.S., Rod Dunbar, P., Romero, P., Chen, J.L., and Cerundolo, V. (1998). High frequency of skin-homing melanocyte-specific cytotoxic T lymphocytes in autoimmune vitiligo. J. Exp. Med. *188*, 1203–1208.

Okamoto, T., Irie, R.F., Fujii, S., Huang, S.K., Nizze, A.J., Morton, D.L., and Hoon, D.S. (1998). Anti-tyrosinase-related protein-2 immune response in vitiligo patients and melanoma patients receiving active-specific immunotherapy. J. Invest. Dermatol. *111*, 1034–1039.

Ongenae, K., Van Geel, N., and Naeyaert, J.M. (2003). Evidence for an autoimmune pathogenesis of vitiligo. Pigment Cell Res. *16*, 90–100.

Ratsep, R., Kingo, K., Karelson, M., Reimann, E., Raud, K., Silm, H., Vasar, E., and Koks, S. (2008). Gene expression study of IL10 family genes in vitiligo skin biopsies, peripheral blood mononuclear cells and sera. Br. J. Dermatol. *159*, 1275–1281.

Ruiz-Arguelles, A., Brito, G.J., Reyes-Izquierdo, P., Perez-Romano, B., and Sanchez-Sosa, S. (2007). Apoptosis of melanocytes in vitiligo results from antibody penetration. J. Autoimmun. *29*, 281–286.

Schallreuter, K.U., Lemke, R., Brandt, O., Schwartz, R., Westhofen, M., Montz, R., and Berger, J. (1994a). Vitiligo and other diseases: coexistence or true association? Hamburg study on 321 patients. Dermatology *188*, 269–275.

Schallreuter, K.U., Wood, J.M., Pittelkow, M.R., Gutlich, M., Lemke, K.R., Rodl, W., Swanson, N.N., Hitzemann, K., and Ziegler, I. (1994b). Regulation of melanin biosynthesis in the human epidermis by tetrahydrobiopterin. Science *263*, 1444–1446.

Swope, V.B., Sauder, D.N., Mckenzie, R.C., Sramkoski, R.M., Krug, K.A., Babcock, G.F., Nordlund, J.J., and Abdel-Malek, Z.A. (1994). Synthesis of interleukin-1 alpha and beta by normal human melanocytes. J. Invest. Dermatol. *102*, 749–753.

Virador, V.M., Kobayashi, N., Matsunaga, J., and Hearing, V.J. (1999). A standardized protocol for assessing regulators of pigmentation. Anal. Biochem. *270*, 207–219.

Wang, C.Q., Cruz-Inigo, A.E., Fuentes-Duculan, J., Moussai, D., Gulati, N., Sullivan-Whalen, M., Gilleaudeau, P., Cohen, J.A., and Krueger, J.G. (2011). Th17 cells and activated dendritic cells are increased in vitiligo lesions. PLoS ONE *6*, e18907.

Wilson, N.J., Boniface, K., Chan, J.R. et al. (2007). Development, cytokine profile and function of human interleukin 17-producing helper T cells. Nat. Immunol. *8*, 950–957.

Supporting information

Additional Supporting Information may be found in the online version of this article:

Figure S1. Coculture of helper T cells and melanocytes, and measurement of the expression of melanogenic markers.

Please note: Wiley-Blackwell are not responsible for the content or functionality of any supporting materials supplied by the authors. Any queries (other than missing material) should be directed to the corresponding author for the article.

The American Journal of Pathology, Vol. 180, No. 1, January 2012

DOI: 10.1016/j.ajpath.2011.09.013

Growth Factors, Cytokines, and Cell Cycle Molecules

Blockade of Interleukin-6 Receptor Alleviates Disease in Mouse Model of Scleroderma

Shun Kitaba,* Hiroyuki Murota,* Mika Terao,* Hiroaki Azukizawa,* Fumitaka Terabe,† Yoshihito Shima,‡ Minoru Fujimoto,† Toshio Tanaka,‡ Tetsuji Naka,† Tadamitsu Kishimoto,§ and Ichiro Katayama*

From the Department of Dermatology, Course of Integrated Medicine and the Department of Respiratory Medicine, Allergy and Rheumatic Diseases,‡ Graduate School of Medicine, Osaka University, Osaka; the Laboratory for Immune Signal,† National Institute of Biomedical Innovation, Osaka; and the Laboratory of Immune Regulation,§ Osaka University Graduate School of Frontier Biosciences, Osaka, Japan*

Activation of fibroblasts by interleukin-6 (IL-6) is implicated in the pathogenesis of scleroderma, suggesting that the inhibition of fibroblast activation may be a promising scleroderma treatment. In this study, we used an IL-6 blocking antibody (Ab) and *Il-6* knockout (Il-6KO) mice to examine the role of IL-6 in the bleomycin (BLM)-induced mouse model of scleroderma. BLM was administered to C57BL/6 and *Il-6*KO mice to induce dermal sclerosis. BLM-treated and control phosphate-buffered saline-treated mice were treated with anti-mouse IL-6 receptor monoclonal Ab (MR16-1). Disease severity was evaluated by measuring dermal thickness and skin hardness, by counting the numbers of α-smooth muscle actin-positive cells and mast cells, and by examining the cutaneous draining lymph nodes. C57BL/6 mice with BLM induced scleroderma had elevated serum IL-6 levels and more severe dermal sclerosis than *Il-6*KO mice. Weekly administration of MR16-1, but not control Ab, prevented and improved dermal sclerosis, and also attenuated swelling of the draining lymph nodes. MR16-1 suppressed α-smooth muscle actin induction in IL-6–stimulated *Il-6*KO fibroblasts. Our results indicate that IL-6 contributes to BLM induced dermal sclerosis and that IL-6 receptor–specific monoclonal Ab may improve the symptoms of scleroderma by suppressing fibroblast activation. *(Am J Pathol 2012, 180:165–176; DOI: 10.1016/j.ajpath.2011.09.013)*

Patients with scleroderma frequently experience broad area skin sclerosis and internal organ involvement including pulmonary fibrosis, esophageal dysfunction, pulmonary arterial hypertension, renal crisis, and heart failure.[1] These symptoms dramatically affect the prognosis for scleroderma patients. Autoaggressive immunological activation and continuous activation of fibroblasts are the key components of scleroderma, yet the mechanisms underlying these are incompletely understood.

Several lines of evidence indicate that interleukin (IL)-6 contributes to the disease process in scleroderma. Serum IL-2, IL-4, IL-6, and tumor necrosis factor α levels are elevated in scleroderma.[2–6] Increased serum IL-6 levels are also observed in both scleroderma mouse models: the bleomycin (BLM)-induced scleroderma mouse and the type 1 tight-skin mouse (*Tsk1/+*).[7,8] At the cellular level, IL-6–producing T helper type 2 clones contribute to anti-DNA topoisomerase I autoantibody, a key autoantibody in scleroderma.[9] The point of action of IL-6 in scleroderma remains controversial, with some evidence suggesting the final maturation step of B cells[10] and/or activation of fibroblasts.[11–13] Thus, although the specific function of IL-6 in the pathogenesis of scleroderma remains unclear, there is ample evidence that inhibition of IL-6–mediated signaling might be a route to better treatment for scleroderma.

In this study, we used the BLM-induced scleroderma mouse model to demonstrate the importance of IL-6 in pathogenesis of scleroderma and to evaluate the effect of anti-mouse IL-6 receptor monoclonal antibody. We have examined whether MR16-1 acts directly on dermal fibroblasts by investigating the induction of myofibroblasts *in vitro*. We also examined the tissue of scleroderma patients treated with tocilizumab, a humanized monoclonal antibody (Ab) against the IL-6 receptor used to treat rheumatoid arthritis or Castleman's disease.[14] Patients

Supported by the Program for Promotion of Fundamental Studies in Health Sciences of the National Institute of Biomedical Innovation.

Accepted for publication September 21, 2011.

Disclosure: T.K. holds a patent for tocilizumab. All other authors have no conflicts of interest to declare.

Address for reprint requests: Hiroyuki Murota, M.D., Ph.D., 2-2, Yamadaoka, Suita-Shi, Osaka, Japan 565-0871. E-mail: h-murota@derma.med.osaka-u.ac.jp.

with intractable scleroderma treated with tocilizumab were previously reported to show marked amelioration of dermal sclerosis.[15] Our results indicate that IL-6 induces dermal sclerosis via direct activation of dermal fibroblasts and that biomolecular targeting to suppress IL-6 might be a promising therapeutic approach for scleroderma.

Materials and Methods

Dermal Fibroblast Isolation and Culture

The dermis was collected and separated from the epidermis as described previously.[4,16] Briefly, newborn wild-type and *Il-6* knockout (KO) mouse pups (age 2 to 4 days) were sacrificed and rinsed in 70% ethanol. The skin was excised and treated with 4 mg/mL of dispase (Gibco, Invitrogen, Paisley, UK) for 1 hour at 37°C. The dermis was then separated from the epidermis, placed in phosphate-buffered saline (PBS) + 0.05% type-1 collagenase (Sigma-Aldrich, St. Louis, MO), and incubated at 37°C for 30 minutes with vigorous agitation to prepare single cells. After filtration, cells were resuspended in Dulbecco's modified Eagle's medium + 10% fetal bovine serum and incubated at 37°C and 5% CO_2.

The primary *Il-6*KO fibroblasts were passaged once or twice and used for subsequent experiments. Cells were confirmed to have the classical morphology (long spindle shape) of fibroblasts.

Patients and Skin Samples

This study included two scleroderma patients treated with tocilizumab and three scleroderma patients not treated with tocilizumab. Two scleroderma patients were treated with 8 mg/kg of tocilizumab monthly for 6 months with the permission of the Ethics Committee of Osaka University Hospital and after receipt of informed consent. Detailed patient information was described previously.[15] Skin samples were obtained from patients before and after treatment. Written informed consent was obtained from all patients before skin biopsy.

Immunofluorescent Staining

Wild-type (C57BL/6) and *Il-6*KO fibroblasts were cultured to semiconfluence in 350-mm culture plates. The cultures were fixed in 4% paraformaldehyde at room temperature for 10 minutes and permeabilized with 0.5% Triton in PBS for 5 minutes. The primary Abs used were mouse monoclonal anti–α-smooth muscle actin Ab (1:100, α-SMA; Dako-Cytomation, Carpinteria, CA) , After 1 hour incubation, cells were stained for 30 minutes with Alexa Fluor 488 anti-mouse IgG secondary Ab to α-SMA (Invitrogen, Carlsbad, CA) and Hoechst 33342 (Molecular Probes, Eugene, OR). Mouse IgG_{2a} (Dako-Cytomation, Carpinteria, CA) was used as a control for nonspecific staining.

Paraffin-embedded sections derived from scleroderma patients treated with 6 months of tocilizumab or 6 months of prednisolone, and redundant tissue from surgical specimens were deparaffinized and hydrated. Skin sections derived from patients were brought to a boil in 10 mmol/L sodium citrate buffer (pH 6.0) and then maintained at a subboiling temperature for 10 minutes. After blocking with 5% normal goat serum (Vector Laboratories, Burlingame, CA) in PBST, they were double-stained with mouse monoclonal anti–α-SMA Ab (Dako-Cytomation) and rabbit monoclonal phospho-p44/42 MAPK Ab (Cell Signaling, Beverly, MA). Secondary antibodies were as follows: anti-mouse Alexa Fluor 488 for α-SMA Ab and biotinylated anti-rabbit IgG (Vector Laboratories) plus DyLight594-conjugated Streptavidin (Jackson ImmunoResearch Laboratories, West Grove, PA) for phospho-p44/42 MAPK Ab. Images of immunolabeled sections were captured with a BZ-8000 microscope (Keyence, Osaka, Japan).

Table 1. Effect of MR16-1 on BLM-Induced Dermal Sclerosis in a Prevention Model

	Thickness (mm)			Hardness (Arbitrary)		
	1st (n = 4)	2nd (n = 4)	3rd (n = 4)	1st (n = 4)	2nd (n = 4)	3rd (n = 4)
PBS						
Control Ab	0.137 ± 0.016	0.10 ± 0.01	0.123 ± 0.010	7.09 ± 2.17	6.14 ± 0.72	4.86 ± 1.05
MR16-1	0.11 ± 0.01	0.111 ± 0.011	0.122 ± 0.013	8.91 ± 2.59	6.45 ± 1.49	4.92 ± 0.77
% Change						
Each experiment	81.82	106.33	98.65	125.64	104.91	101.15
Mean ± SE		95.60 ± 7.238			110.6 ± 7.614	
BLM						
Control Ab	0.33 ± 0.04*	0.36 ± 0.05*	0.30 ± 0.07*	24.14 ± 5.58*	16.61 ± 1.90*	9.93 ± 1.51*
MR16-1	0.22 ± 0.03†‡	0.29 ± 0.02‡§	0.16 ± 0.03†	15.47 ± 4.52	8.53 ± 0.80†	5.92 ± 0.49†
% Change						
Each experiment	67.09	81.29	52.22	64.08	51.33	59.59
Mean ± SE		66.89 ± 8.39			58.34 ± 3.74	

(*table continues*)

Values are mean ± SD. To quantify the impact of BLM treatment, % changes were calculated as follows: (evaluative consequences of BLM treatment/that of PBS treatment) × 100 (%).

*P < 0.01 PBS+Control Ab versus BLM+Control Ab.

†P < 0.01 BLM+Control Ab versus BLM+MR16-1.

‡P < 0.01 PBS+MR16-1 versus BLM+MR16-1.

§P < 0.05 BLM+Control Ab versus BLM+MR16-1.

HPS, high-power field.

Western Blot Analysis

Wild-type and *Il-6*KO fibroblasts were prepared as described above and cultured to semiconfluence in 100-cm^2 culture plates. Before treatment, fibroblast cultures were washed twice with PBS, and culture media were replaced with low-serum (0.1%fetal bovine serum) Dulbecco's modified Eagle's medium containing 60 IU/mL penicillin, 100 IU/mL streptomycin, and 4 mmol/L glutamine. Low-serum medium was necessary to maintain viability of primary fibroblasts overnight.

Following 12 hours incubation in low-serum medium, treatments were applied to the cultures in fresh low-serum Dulbecco's modified Eagle's medium. Semiconfluent cultures were treated with 10 ng/mL of MR16-1 or 10 μmol/L of PD98058 (Calbiochem, San Diego, CA) for 3 hours, and then 10 ng/mL of recombinant mouse IL-6 (R&D Systems, Minneapolis, MN) was added to the cultures for 24 hours. At indicated time points, culture plates were rinsed twice with ice-cold PBS, and total cell protein was collected in 500 μL of lysis buffer [50 mmol/L Tris-HCl (pH 7.6), 150 mmol/L NaCl, 1% deoxycholic acid, 0.1% sodium dodecyl sulfate, 1% Triton X-100, 1 mmol/L sodium orthovanadate, and protease inhibitor cocktail]. Western blot analysis was performed as previously described.[4] Ten micrograms of protein were fractionated on SDS-polyacrylamide gels and transferred onto PVDF membranes (Bio-Rad, Hercules, CA). Nonspecific protein binding was blocked by incubating the membranes in 5% w/v nonfat milk powder in TBST [50 mmol/L Tris-HCl (pH 7.6), 150 mmol/L NaCl, and 0.1% v/v Tween-20]. The membranes were incubated with mouse monoclonal anti–α-SMA (Dako-Cytomation) Ab at a dilution of 1:1000 overnight at 4°C or with mouse monoclonal anti–β-actin (Sigma-Aldrich) at a dilution of 1:5000 for 30 minutes at room temperature. After three 5-minute washes in TBST, membranes were incubated with horseradish peroxidase–conjugated anti-mouse Ab at a dilution of 1:10,000 for 60 minutes at room temperature. Protein bands were detected using the ECL Plus kit (GE Healthcare, Little Chalfont, UK). Western blot quantification was performed with ImageJ software (NIH, Bethesda, MD) and used to visualize fold expression differences between these treatment groups.

Mice and Induction of Skin Sclerosis

Six-week-old female mice were used in all experiments. C57BL/6 mice were purchased from Japan Clea (Osaka, Japan). Mutant C57BL/6 mice rendered null for IL-6 were described previously[17] and were purchased from the National Institute of Biomedical Innovation (Osaka, Japan). Mice were maintained in our pathogen-free animal facility. All animal care was in accordance with the institutional guidelines of Osaka University. BLM (Nippon Kayaku, Tokyo, Japan) was dissolved in PBS at a concentration of 1 mg/mL and sterilized by filtration. BLM (0.1 mg/100 μL) was injected subcutaneously into the shaved back of the mice daily for 4 weeks with a 27-gauge needle as described by Yamamoto et al.[7] Control mice received 100 μL of PBS instead.

RNA Isolation and Real-Time PCR

Sections of skin lesions and the cutaneous draining lymph nodes (LNs) were removed 1 day after the final injection. Total RNA was isolated using the SV Total RNA Isolation System (Promega, Madison, WI) and reverse transcribed into complementary DNA.

IL-6 expression was measured using the Power SYBR Green PCR Master Mix (Applied Biosystems, Foster City, CA) according to the manufacturer's protocol. Glyceraldehyde-3-phosphate dehydrogenase (GAPDH) was used to normalize the mRNA. Sequence-specific primers were: IL-6, sense 5′-ACACACTGGTTCTGAGGGAC-3′, antisense 5′-TACCACAAGGTTGGCAGGTG-3′; GAPDH,

Table 1. *Continued*

α-SMA–Positive Cells (Cells/HPS)			Mast Cells (Cells/HPS)		
1st (n = 4)	2nd (n = 4)	3rd (n = 4)	1st (n = 4)	2nd (n = 4)	3rd (n = 4)
6.00 ± 4.08	3.50 ± 1.29	8.75 ± 1.50	12.50 ± 4.51	21.67 ± 3.06	31.50 ± 5.45
5.00 ± 1.73	4.00 ± 1.41	10.00 ± 4.16	11.00 ± 1.83	17.33 ± 6.11	29.75 ± 3.50
83.33	114.29	114.29	88.00	80.00	94.44
	104.0 ± 10.32			87.48 ± 4.177	
14.00 ± 1.83*	14.50 ± 4.93*	27.75 ± 0.96*	46.50 ± 8.43*	35.33 ± 5.69*	67.25 ± 5.85*
10.00 ± 1.41	7.00 ± 1.82§	15.25 ± 2.75†	20.25 ± 4.99†	25.00 ± 2.00	29.50 ± 6.19†
71.43	48.28	54.95	43.55	70.75	43.87
	58.22 ± 6.88			52.72 ± 9.02	

Table 2. Effect of MR16-1 on BLM-Induced Dermal Sclerosis in a Treatment Model

	Thickness (mm)		Hardness (arbitrary)		α-SMA–positive cells (cells/HPS)		Mast cells (cells/HPS)	
	1st (n = 4)	2nd (n = 3)	1st (n = 4)	2nd (n = 3)	1st (n = 4)	2nd (n = 3)	1st (n = 4)	2nd (n = 3)
PBS								
Control Ab	0.14 ± 0.02	0.12 ± 0.03	4.80 ± 0.47	6.19 ± 1.29	3.75 ± 1.50	2.33 ± 0.58	13.50 ± 1.73	19.67 ± 2.52
MR16-1	0.12 ± 0.01	0.107 ± 0.006	4.67 ± 0.47	5.68 ± 0.43	3.33 ± 0.56	2.67 ± 1.15	15.33 ± 1.15	21.00 ± 2.00
% Changes	83.64	86.49	97.22	91.78	88.88	106.78	113.58	106.78
BLM								
Control Ab	0.30 ± 0.03*	0.29 ± 0.03*	9.34 ± 1.58*	9.81 ± 1.17†	10.00 ± 2.58*	7.67 ± 0.58*	37.75 ± 2.50*	54.67 ± 8.39*
MR16-1	0.21 ± 0.05‡‖	0.18 ± 0.03§¶	5.46 ± 0.62¶	5.41 ± 0.77¶	5.50 ± 1.29¶	4.00 ± 1.00¶	27.00 ± 2.16§¶	37.00 ± 6.56‡‖
% Changes	70.00	62.50	58.46	55.12	55.00	52.17	71.52	67.68

Mean ± SD is presented. To quantify the impact of MR16-1treatment, % changes were calculated as follows: (evaluative consequences of MR16-1 treatment/that of PBS treatment) × 100 (%).
*P < 0.01 PBS+Control Ab versus BLM+Cont. Ab.
†P < 0.05 PBS+Control Ab versus BLM+Cont. Ab.
‡P < 0.05 BLM+Control Ab versus BLM+MR16-1.
§P < 0.01 PBS+MR16-1 versus BLM+MR16-1.
¶P < 0.01 BLM+Control Ab versus BLM+MR16-1
‖P < 0.05 PBS+MR16-1 versus BLM+MR16-1.
HPS, high-power field.

sense 5′-TGTCATCATACTTGGCAGGTTTCT-3′, antisense 5′-CATGGCCTTCCGTGTTCCTA-3′. Real-time PCR (40 cycles of denaturing at 92°C for 15 seconds and annealing at 60°C for 60 seconds) was run on an ABI 7000 Prism Detection System (Applied Biosystems).

Mouse IL-6 Receptor–Specific Monoclonal Antibody Treatment

Rat anti-mouse IL-6 receptor monoclonal Ab (clone MR16-1, rat $IgG_{1)}$ described previously[18] was provided by Chugai Pharmaceutical (Shizuoka, Japan). Purified rat IgG_1 (isotype-matched control Ab) (Cappel, MP Biomedicals, Solon, OH) was administered as a control. Preventive and therapeutic administration methods are discussed later. Percentage to control values were calculated as follows: (mean actual value/mean control value) × 100.

Enzyme-Linked Immunosorbent Assay of IL-6 Levels in Sera and Conditioned Media

Serum samples were obtained from mice injected with BLM or PBS for 28 days. Conditioned media were obtained from cultured primary dermal fibroblasts of wild-type and *Il-6*KO mice after 24 hours. Serum and conditioned media IL-6 level was measured by enzyme-linked immunosorbent assay using a commercial kit (R&D Systems, Minneapolis, MN) with a detection limit of 7.8 pg/mL.

Vesmeter Measurements

Skin hardness was measured using a Vesmeter.[19] Mice were sacrificed 1 day after the final injection. Skin hardness was measured three times at the injection area, avoiding the backbone of the mouse. Skin hardness was expressed as the area of the depression caused by the

Table 3. Attenuated BLM-Induced Dermal Sclerosis in *Il-6*KO Mice

	Thickness (mm)		Hardness (arbitrary)		α-SMA–positive cells (cells/HPS)		Mast cells (cells/HPS)	
	1st (n = 4)	2nd (n = 3)	1st (n = 4)	2nd (n = 3)	1st (n = 4)	2nd (n = 3)	1st (n = 4)	2nd (n = 3)
WT								
PBS	0.112 ± 0.013	0.14 ± 0.04	4.91 ± 0.38	5.46 ± 0.93	4.75 ± 1.50	8.00 ± 2.00	18.00 ± 3.16	28.33 ± 4.51
BLM	0.32 ± 0.02*	0.29 ± 0.06†	12.38 ± 0.81*	9.69 ± 0.51*	19.75 ± 5.74*	23.33 ± 6.11*	40.25 ± 2.22*	63.33 ± 9.87*
% Change	282.85	203.13	251.99	177.28	415.79	291.67	223.61	223.53
Il-6								
PBS	0.111 ± 0.010	0.12 ± 0.01	5.37 ± 0.48	5.12 ± 0.71	4.00 ± 1.41	6.67 ± 2.52	17.75 ± 2.5	29.5 ± 0.71
BLM	0.22 ± 0.03‡§	0.17 ± 0.03‡	7.14 ± 0.96‡¶	5.85 ± 0.21‡	9.50 ± 4.43‖	13.00 ± 1.73‖	22.75 ± 4.79‡	34.00 ± 7.00‖
% Change	195.71	133.81	132.87	114.21	237.50	195.00	128.17	115.25

Mean ± SD was presented. To quantify the impact of BLM treatment, % changes were calculated as follows: (evaluative consequences of BLM treatment/that of PBS treatment) × 100 (%).
*P < 0.01 WT with PBS versus WT with BLM.
†P < 0.05 WT with PBS versus WT with BLM.
‡P < 0.01 WT with BLM versus *Il-6*KO with BLM.
§P < 0.01 *Il-6*KO with PBS versus *Il-6*KO with BLM.
¶P < 0.05 *Il-6*KO with PBS versus *Il-6*KO with BLM.
‖P < 0.05 WT with BLM versus *Il-6*KO with BLM.
HPS, high-power field; WT, wild-type.

Table 4. Number of Lymph Node Cells in the Scleroderma Mouse Model

	1st experiment (total number/lymph node, × 10^7)			2nd experiment (total number/lymph node, × 10^6)		
	PBS	BLM	% Change	PBS	BLM	% Change
WT						
Control Ab	0.97 ± 0.21 (n = 3)	2.17 ± 0.31* (n = 3)	222.61	1.90 ± 0.41 (n = 4)	3.55 ± 0.21* (n = 4)	186.73
MR16-1	0.76 ± 0.02 (n = 3)	0.80 ± 0.12† (n = 3)	105.29	1.85 ± 0.18 (n = 4)	1.85 ± 0.34† (n = 4)	99.84
Il-6KO						
WT	0.81 ± 0.18 (n = 3)	1.53 ± 0.40‡ (n = 3)	190.03	2.36 ± 0.26 (n = 3)	3.71 ± 0.61‡ (n = 3)	157.42
Il-6KO	0.66 ± 0.26 (n = 3)	0.54 ± 0.09§ (n = 3)	82.73	1.97 ± 0.67 (n = 3)	2.20 ± 0.29§ (n = 3)	111.51

Mean ± SD was presented. To quantify the impact of BLM treatment, % changes were calculated as follows: (evaluative consequences of BLM treatment/that of PBS treatment) × 100 (%).
*P < 0.01 PBS+Control Ab versus BLM+Cont. Ab.
†P < 0.01 BLM+Control Ab versus BLM+MR16-1.
‡P < 0.05 PBS+Control Ab versus BLM+Cont. Ab.
§P < 0.05 BLM+Control Ab versus BLM+MR16-1.

probe divided by the pressure of the indenter in a connected computer.

Histopathological Analysis

The back skin was removed 1 day after the final injection. Skin pieces were fixed with 10% formaldehyde for 24 hours, embedded in paraffin, and sectioned at 3-μm thickness using a microtome. Sections were stained with hematoxylin and eosin (H&E). Dermal thickness (measured from the epidermal–dermal junction to dermal–fat junction) was determined at ×100 magnification at three randomly selected sites in each animal. Mast cells were identified in 3-μm deparaffinized sections stained with 1% Toluidine Blue, and mast cells were counted in 10 randomly selected sites under × 400 power using light microscopy.

Immunohistochemical Analysis of α-SMA

Sections were cut and processed as described above. For immunohistochemical analysis, sections were deparaffinized by passage through xylene and graded ethanols. Next, endogenous peroxide was blocked using 3% H_2O_2 in methanol for 5 minutes. Slides were blocked with 2% bovine serum albumin for 10 minutes, and stained with primary Ab (anti–α-SMA Ab 1:100 dilution) for 60 minutes. After washing with PBS containing 0.05% Triton, they were developed using Dako ChemMate Envision Kit/horseradish peroxidase (Dako-Cytomation) for 30 minutes, and counterstained with hematoxylin. α-SMA–positive fibroblastic cells were counted in 10 randomly selected sites under × 400 power using light microscopy.

Flow Cytometric Analysis

The skin draining LNs were assessed as a mixture to facilitate analysis. One day after the final infection, mice were sacrificed, and axillary, brachial, and inguinal LNs from each mouse were combined. Cell suspensions of LN cells were stained with antibodies against the following cell surface antigens: CD4, CD8, B220, CD11c, F4/80, and PDCA1 (BD Biosciences, San Jose, CA). Stained cells were analyzed by flow cytometry using a FACSCalibur flow cytometer (BD Biosciences).

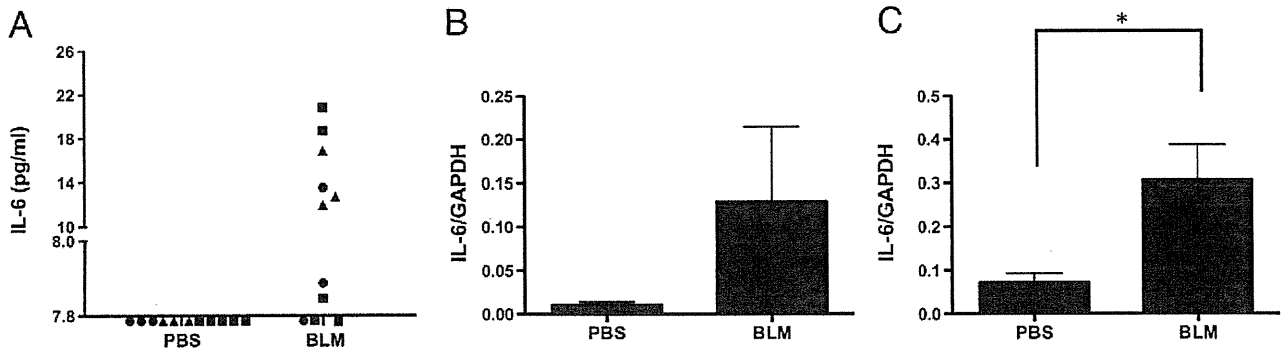

Figure 1. IL-6 production in BLM-treated C57BL/6 mice. C57BL/6 mice treated with PBS or BLM for 4 weeks. **A:** Serum samples were obtained from mice injected with 1 mg/mL BLM (100 μL/day, n = 11) or PBS (100 μL/day, n = 11) for 4 weeks. The data presented are from three experiments of three to five mice each for a total of 11 BLM-treated mice and 11 PBS-treated mice. Serum IL-6 level was measured by enzyme-linked immunosorbent assay using a kit with a detection limit of 7.8 pg/mL (R&D Systems). The mice from different experiments were gave different symbols [box (n = 5), circle (n = 3), and triangles (n = 3)]. Each symbol represents one IL-6 measurement for a single mouse, and symbols below 7.8 pg/mL indicate mice for which IL-6 was below the limit of detection. enzyme-linked immunosorbent assays were run in duplicate for all mice, with similar results. **B** and **C:** Expression of IL-6 mRNA was measured by real-time PCR. RNA was extracted from skin lesions (**B**) and cutaneous draining LNs (**C**) from C57BL/6 mice treated with PBS (n = 3) or BLM (n = 3) for 4 weeks. Data were normalized to the GAPDH internal control. Bars represent mean ± SD. *P < 0.05, unpaired t-test. Data in B and C are from one of two independent experiments that gave similar results. The IL-6/GAPDH data (mean ± SD) for skin lesions (**B**) were as follows: first experiment (n = 3), PBS: 0.011 ± 0.006, BLM: 0.129 ± 0.148 (P = 0.2391); second experiment (n = 3), PBS: 0.142 ± 0.070, BLM: 0.441 ± 0.283 (P = 0.1495). The IL-6/GAPDH data (mean ± SD) for cutaneous draining LNs (**C**) were as follows: first experiment (n = 3), PBS: 0.071 ± 0.038, BLM: 0.306 ± 0.141 (P = 0.0493), second experiment (n = 3), PBS: 0.083 ± 0.0.067, BLM: 0.430 ± 0.175 (P = 0.0321).

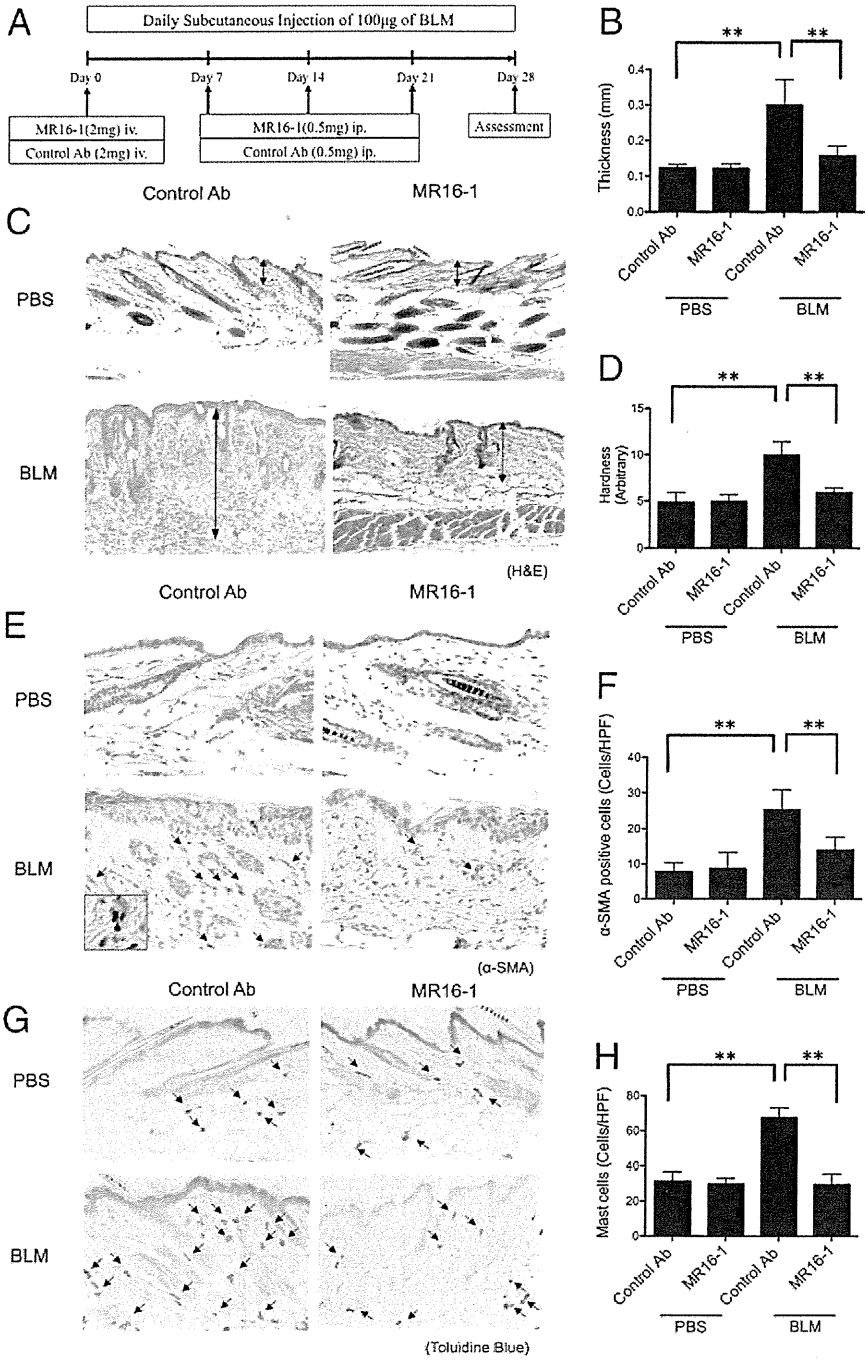

Figure 2. Effect of MR16-1 on BLM-induced dermal sclerosis in a prevention model. **A:** Experimental protocol for prevention of BLM-induced dermal sclerosis by administration of MR16-1 or control Ab to either PBS- or BLM-treated mice ($n = 4$ for each group). Histological and physical examination of the lesional skin was performed on the final day (day 28) of the protocol. **B:** Measurements of dermal thickness ($n = 4$ for each group). **C:** H&E staining of specimens derived from PBS-, or BLM-injected mice treated with MR16-1 or control Ab (original magnification, ×40). The length of each **two-headed arrow** indicates the measurement region of dermal thickness. **D:** Skin hardness measurements obtained using a Vesmeter ($n = 4$ for each group). **E:** Immunohistochemical staining for α-SMA. **Arrows** indicate α-SMA–positive fibroblasts (original magnification, ×100). **Inset** photo shows higher magnification (×200) of α-SMA–positive fibroblasts. **F:** The number of α-SMA–positive fibroblasts per high-power field (HPF, ×400) was determined by observation of 10 random grids. The value graphed is the average of the observation of 10 grids for each of the four mice in the group. **G:** Results of Toluidine Blue staining. **Arrows** indicate the metachromatically stained mast cells (original magnification, ×100). **H:** The number of mast cells per HPF (×400) was determined by observation of 10 random grids. The value graphed is the average of the observation of 10 grids for each of the four mice in the group. **C**, **D**, **F**, and **H:** Bars represent mean ± SD. $^{*}P < 0.05$, $^{**}P < 0.01$, one-way analysis of variance and Bonferroni post hoc multiple comparison. Data presented are from the third of three independent experiments with similar results presented in Table 1.

Computation Methods and Statistical Analysis

All data except change ratios are expressed as mean values ± standard deviations (SDs). To quantify the impact of MR16-1-and BLM treatment, change ratios (%) are calculated for single experiments in Table 1–4. Percent changes in Table 1 are averaged for three experiments and expressed as mean values ± standard errors (SEs). Unpaired *t*-test was used to examine the statistical value between two variable quantities. One-way analysis of variance and the Bonferroni post hoc multiple comparison procedure were used to determine the level of significance between each of three or more variable quantities.

Results

Elevated IL-6 in Mice with BLM-Induced Scleroderma

We first determined the serum concentration and mRNA expression of IL-6 in the skin and cutaneous draining LNs from mice with skin fibrosis induced by subcutaneous